Evapotranspiration partition using the multiple energy balance version of the ISBA-A-g_s land surface model over two irrigated crops in a semi-arid Mediterranean region (Marrakech, Morocco)

Aouade Ghizlane[1], Jarlan Lionel[2,*], Ezzahar Jamal[3,4], Er-raki Salah[5,4], Napoly Adrien[6], Benkaddour Abdelfattah[1], Khabba Said[7,4], Boulet Gilles[2], Garrigues Sébastien[8,9], Chehbouni Abdelghani[2,4], Boone Aaron[6]

[1]Laboratoire des Géo- ressources/LMI TREMA, Faculté des Sciences et Techniques, Université Cadi Ayyad, Marrakech, Maroc.
[2]Centre d'Etudes Spatiales de la Biosphère (CESBIO)/IRD, Toulouse, France.
[3]Département GIRT/Laboratoire MISC, Ecole Nationale des Sciences Appliquées, Université Cadi Ayyad, Safi, Maroc.
[4]CRSA, Center of Remote Sensing Application, Mohammed VI Polytechnic University UM6P, Benguerir, Morocco.
[5]LP2M2E, Faculté des Sciences et Techniques, Université Cadi Ayyad, Marrakech.

[6]Centre National de Recherches Météorologiques (CNRM), Météo-France/CNRS, Toulouse, France.

[7]LMME, Département de physique, Faculté des Sciences Semlalia, Université Cadi Ayyad, Marrakech, Maroc
[8]EMMAH, INRA, Université d'Avignon et des Pays de Vaucluse, Avignon, France
[9]Centre for Ecology and Hydrology (CEH) Wallingford, UK

Correspondence to: Lionel Jarlan (lionel.jarlan@cesbio.cnes.fr)

Abstract. The main objective of this work is to question the representation of the energy budget in surface-vegetation-atmosphere transfer (SVAT) models for the prediction of the turbulent fluxes in the case of irrigated crops with a complex structure (row) and under strong transient hydric regimes due to irrigation. To this objective, the Interaction Soil-Biosphere-Atmosphere (ISBA-A-gs) is evaluated over a complex open olive orchard and, for comparison purpose, on a winter wheat field taken as an example of homogeneous canopy. The initial version of ISBA-A-gs based on a composite energy budget (named hereafter ISBA-1P for 1 patch) is compared to the new multiple energy balance (MEB) version of ISBA representing a double source arising from the vegetation located above the soil layer. In addition, a patch representation corresponding to two-adjacent uncoupled source schemes (ISBA-2P for 2 patches) is also considered for the Olive orchard. Continuous observations of evapotranspiration (ET) with an eddy-covariance system and plant transpiration (T_r) with Sapflow and isotopic methods were used to evaluate the three representations. A preliminary sensitivity analyses showed a strong sensitivity to the parameters related to turbulence in the canopy introduced in the new ISBA-MEB version. Over wheat, the ability of the single and dual-source configuration to reproduce the composite soil-vegetation heat fluxes was very similar: the RMSE differences between ISBA-1P, -2P and -MEB did not exceed 10 W/m^2 for the latent heat flux. These results showed that a composite energy balance on homogeneous covers is sufficient to reproduce the total convective fluxes. The two configurations are also fairly close to the isotopic observations of transpiration in spite of a light underestimation

(overestimation) of ISBA-1P (ISBA-MEB). On the Olive Orchard, contrasting results are obtained. The dual source configurations including both the uncoupled (ISBA-2P) and the coupled (ISBA-MEB) representations outperformed the single source version (ISBA-1P) with slightly better results for ISBA-MEB in predicting both total heat fluxes and evapotranspiration partition. Concerning plant transpiration in particular, the coupled approach ISBA-MEB provides better results than ISBA-1P and, to a lesser extent ISBA-2P with RMSEs of 1.60, 0.90, 0.70 mm/day and R^2 of 0.43, 0.69 and 0.70 for ISBA-1P, -2P and MEB respectively. In addition, it is shown that the acceptable predictions of composite convective fluxes by ISBA-2P for the Olive orchard are obtained for the wrong reasons as neither of the two patches is in agreement with the observations because of a bad spatial distribution of the roots and of a lack of incoming radiation screening for the bare soil patch. This work shows that composite convection fluxes predicted by the SURFEX platform as well as partition of evapotranspiration in a highly transient regime due to irrigation is improved for moderately open tree canopies by the new coupled dual-source ISBA-MEB model. It also points out the need for further local scale evaluation on different crops of various geometry (more open rainfed or denser intensive olive orchard) to provide adequate parameterization to global data base such as ECOCLIMAP-II in the view of a global application of the ISBA-MEB model.

Keywords: ISBA model, Evapotranspiration, Crop transpiration, Soil evaporation, eddy-covariance, Sapflow, Stable isotopes, Flood-irrigated crops, Semi-arid region.

1 Introduction

As a major connection linking the water budget and energy balance, evapotranspiration (ET) is a primary process driving the moisture and heat transfers between the land and the atmosphere (Xu et al., 2005; Xu and Singh, 2005; Wang et al., 2013). A good prediction of ET is thus of crucial importance for water recycling processes (Eltahir, 1996) and, in fine, for numerical weather prediction models as well as for climate prediction (Rowntree, 1991). It is also of prime importance for catchment scale hydrology as a major component of the terrestrial water cycle, especially over semi-arid regions. It is, finally, a key variable in agronomy for irrigation scheduling. However, it is also recognized as one of the most uncertain components of the hydro-climatic system (Jasechko et al., 2013). In semi-arid regions of the southern Mediterranean, agriculture consumes about 85% of the total available water and is in continuous expansion (Voltz et al., 2018). With an efficiency lower than 50% due to the use of the traditional flooding systems and to the poor scheduling of irrigation, pushing forward our knowledge of the ET and its partition is also of prime importance for improving the management of agricultural water in this region.

In semi-arid regions, irrigation causes contrasting soil moisture conditions and cools and moistens the surface over and downwind of irrigated areas (Lawston et al., 2015). Irrigation drastically affects the partition of available energy into sensible and latent heat fluxes (Ozdogan et al., 2010), promotes sensible heat advection from the surrounding drier surface (Lei and Yang, 2010) and impacts the partition of ET into plant transpiration T_r, usually associated with plant productivity,

and soil evaporation E that is lost for the plant (Kool et al., 2014). In this context, Hartmann (2016) suggests that transpiration may be more efficient than bare soil evaporation in enhancing the land-atmosphere feedbacks. Indeed, transpiration is associated to longer climate memory than soil evaporation as plant roots can extract water from a deep reservoir and maintains a regular input of water to the atmospheric boundary layer while the small evaporative layer of soils dries out in several days, in particular on semi-arid regions.

Within this context, the micro-meteorological community has developed numerous Soil-Vegetation-Atmosphere Transfer scheme (SVATs) with varying degrees of complexity to estimate ET and its partition (Noilhan and Planton, 1989; Sellers et al., 1996; Noilhan and Mahfouf, 1996; Coudert et al., 2006; Gentine et al., 2007). In parallel, several studies have examined the representation of surface heterogeneity by SVATs and in particular on the surface energy budget. Part of the existing SVATs generally solve a single composite energy balance for the soil and the vegetation and thus calculate a composite temperature. These "mono-source" models have been used successfully on herbaceous, dense and homogenous covers (Kalma and Jupp 1990, Raupach and Finnigan 1988). By contrast, they may not be suited for sparse vegetation (Van Hurk et al., 1995; Blyth and Harding 1995; Boulet et al., 1999) that is a common feature of south Mediterranean crops. Indeed, these covers are characterized by a high heterogeneity in terms of geometry (rank, several layers), especially for tree crops. In the case of irrigated sparse cover, the temperature contrast can be high between, on the one hand, a dry and hot soil interacting directly with the atmosphere and receiving a large fraction of incoming radiation not screened by the vegetation, and, on the other hand, a well-watered vegetation transpiring at its potential rate thanks to irrigation. In addition, the heat sources composing complex crops (soil, tree cover, potential intermediate annual cover …) such as trees are coupled to varying degrees depending on the heterogeneity of the crop. The representation of the intensity of this coupling, and ultimately the performance of the models to reproduce the ET and its partition, is directly related to the structure adopted in the model (single- or dual- source). In particular, it has been shown that a more realistic representation of the energy balance and a better representation of the respective contributions of E and T_r to ET (Shuttleworth and Wallace, 1985; Norman et al., 1995; Béziat et al., 2013; Boulet et al., 2015) could be obtained by solving several separate energy balances for each of the sources. In this context, two types of dual-source models were developed (Lhomme et al., 2012). The coupled or layer approach considers that the canopy is located above the soil layer (Shuttleworth and Wallace, 1985; Shuttleworth and Gurney, 1990, Lhomme et al. 1994, 1997) while for the uncoupled or patch approach, soil and vegetation sources are located next to each other, in parallel. This means that, for the layer representation, exchanges of heat and moisture between the soil and the atmosphere go necessarily through the vegetation layer as it covers completely the ground. By contrast, for the patch representation, soil and vegetation turbulent processes are independent and soil receives the full incoming radiation not screened by the vegetation (Norman et al., 1995; Boulet et al., 2015). The choice between the patch and the layer approach is related to the scale of the surface heterogeneity (Lhomme and Chehbouni, 1994; Boulet et al., 1999; Lhomme et al., 1999; Blyth and Harding, 1995; Lhomme et al., 2012). Roughly, a layer approach should be adopted if the scale of heterogeneity is small while the uncoupled representation is better suited for larger patches allowing for uncoupled surface boundary layers

above each patch. The ratio of vegetation height to the patch size has been proposed as indicator of canopy heterogeneity. Blyth and Harding (1995) and Blyth et al. (1999) found that the coupled model represented better the data in the extreme case of a tiger bush characterized by a ratio of 1/10 than the patch approach. By contrast, Boulet et al. (1999) highlighted that the patch approach was more realistic to predict the energy balance of sparse but relatively homogeneous area dominated by shrub and bushes in the San Pedro Basin. The question thus arises of what is the threshold for choosing one representation from the other? The question is particularly relevant for complex tree crops in the Mediterranean areas such as Olive orchard because a large diversity of field geometry co-exist in the Mediterranean area from the sparser rainfed fields to the denser intensively cropped fields with new tree varieties. Finally, another modeling issue for irrigated agro-system is the highly transient soil moisture regime induced by irrigation and the strong energy switch between latent and sensible heat fluxes at the irrigation time.

The Interaction Soil Biosphere Atmosphere (ISBA) model is part of the SURFace EXternalisée platform (SURFEX) from Météo-France (Masson et al., 2013). It provides the land surface boundary conditions for all the atmospheric models of Météo-France and is used in the operational hydrological system (named SIM for SAFRAN-ISBA-MODCOU; Habets et al., 2008). The standard version of this model (Noilhan and Planton, 1989) uses a single composite soil-vegetation surface energy budget meaning that only a composite soil-vegetation temperature is solved by the model (Noilhan and Planton, 1989; Noilhan and Mahfouf, 1996). Recently, Boone et al. (2017) have developed a multiple energy balance (ISBA-MEB) version that can represent the surface with up to three sources including the snow layer as there are issues in the representation of the snowpack effect on surface temperature for northern latitude forest ecosystems. This new version of ISBA gives a unique opportunity to compare single and dual-source representations of irrigated crops, including complex tree crops, within the same modelling environment (meaning that all other processes are parameterized in the same way). It was evaluated on temperate forested areas (Napoly et al., 2017) without investigating the partition of evapotranspiration.

The main objective of this study is to evaluate the added value of the multiple energy balance in ISBA/SURFEX to simulate surface heat fluxes and the partition of ET into T_r and E over two dominant crop types in the Mediterranean region which are irrigated using the traditional flooding technique. This paper is organized as follows: i) description of the experimental sites and data; ii) description of the model versions and their implementation; iii) sensitivity analysis and model calibration; iiii) comparison of the different ISBA model representation and discussions.

2. Data and Land Surface Model ISBA-A-gs

2.1 Study sites and *in situ* measurements

2.1.1 Study region

The region of study is the Haouz plain located in the Tensift basin (Marrakech, Morocco; Figure 1). The climate of the area is similar to that of the semi-arid Mediterranean zones with hot and dry summers and low precipitation which mostly falls between November and April of each year. The annual rainfall average ranges between 192 mm and 253 mm per year, largely lower than the evaporative demand which is around 1600 mm/year (Jarlan et al., 2015; Chehbouni et al., 2008). In this region, the dominant irrigated crop including arboriculture (olives and oranges) and cereals (wheat) consumes about 85% of available water which comes from groundwater pumping or dams. As reported in Ezzahar et al. (2007a), the majority of the farmers (more than 85%) use the traditional flood irrigation method which causes much loss of water through deeper percolation and soil evaporation. In this study, two flood-irrigated sites of olive orchard and winter wheat have been instrumented with micrometeorological observations.

2.1.2 The olive orchard site

An experiment was set up in an olive orchard site (31°36'N, 07°59'W) named "Agdal" located in the vicinity of Marrakech city during the 2003 and 2004 growing seasons (Figure 1). The site occupies approximately 275 ha of olive with an average height of about 6.5m and a density of 225 trees/ha corresponding to a tree spacing of 7 m and an inter-row of 8 m. The irrigation water are collected after snow melting and stored into two basins. Afterwards, a ditch network is used to divert water from basins to each tree which is surrounded by a small earthen levy. The latter retains irrigation water needed for each tree (Williams et al., 2004). Depending on available manpower, the irrigation of the total area takes approximately 12 days. The farm was properly managed on average during the experimental period apart from a severe water stress that occurred in July 2003. The understory vegetation was removed on a regular basis. In this study, it is assumed that it has a low impact on the micro-meteorological measurements. For more details about the description of the Agdal site and related experimental set-up, the reader can refer to Ezzahar et al. (2007a and 2007b, 2009a and 2009b) and Hoedjes et al. (2007 and 2008).

2.1.3 The winter wheat site

The second experiment was carried out in the irrigated perimeter named "R3" (Figure 1), situated about 45 km east of Marrakech city (31°38'N, 7°38'W). R3 is 2800ha and the main crop is flood-irrigated winter wheat. Depending on the first heavy rainfall during the winter season and climatic conditions, the wheat is generally sown between November and January, and harvested in the end of May. Based on the dam water level at the beginning of each agricultural season, the amount of irrigation water and frequency are managed by the Regional Office of Agricultural Development of the Haouz plain

(ORMVAH). Two wheat fields were instrumented during the seasons 2002-2003 and 2012-2013. The water input applied in the 2003 season was very low compared to the amount provided to the field in 2013. Indeed, only four irrigation events were applied and were not well managed due to the technical constraint of the concrete channel network imposed by ORMVAH. However, the development of the wheat was almost normal. Indeed, Er-Raki et al. (2007) have found that the lengths of growing stages of this wheat compared well with those of another field (six irrigation events) very near to our site. Over the same field, Boulet et al. (2007) have revealed that water stress occurred late in the season when senescence has already started (around May, 6th; the reason is that the farmer stopped the irrigation on April, 21st). More details on the site description and the experimental set-up are provided in Duchemin et al. (2006, and 2008), Ezzahar et al. (2009a), Er-Raki et al.(2007), Le page et al. (2014) and Jarlan et al. (2015).

2.1.4 Data description

Meteorological and micro-meteorological data

Both sites were equipped with a set of standard meteorological instruments to measure air temperature and humidity, wind speed and direction and rainfall. Net radiation and its components were measured above vegetation using two CNR1 radiometers. Over Agdal site, which is an open orchard, CNR1 was placed at 8.5 m height to embrace vegetation and soil radiances by ensuring that the field of view was representative of their respective cover fractions. In addition, two Q7 radiometers were used to measure separately the soil and vegetation net radiations: one was installed over bare soil at 1m and the other over olive tree at 7m. Over the same site, soil and vegetation temperatures were measured using two infrared thermometers (IRTS-Ps), with a 3:1 field of view, at heights of 1m (pointing towards the soil) and 7.15 m (pointing towards the crown of the tree), respectively. Over the wheat site, only one IRTS-Ps installed at 2m was used to measure the composite surface temperature. Soil heat flux density was measured at different depths using soil heat flux plates (HFT3-L, Campbell Scientific Ltd.) over both sites. One can noted that in order to get good average values at soil surface (about 1cm) over olive trees, three HFT3-L were installed at three locations: underneath the canopy (always shaded), in between the trees (mostly sunlit), and in an intermediate position. Also, soil moisture was measured over both sites using time domain reflectometer probes (CS616) installed at different depths. Soil samples were also taken over both sites in order to calibrate the CS616 measurements using the gravimetric technique. All meteorological measurements were sampled at 1 Hz, and 30 min averages were stored.

Finally, sensible and latent heat fluxes were measured using an eddy-covariance method which consisted of a 3D sonic anemometer and krypton hygrometer (KH20) or open-path infra-red gas analyser (LICOR-7500) that measures the fluctuations of the three components of the wind speed, air temperature and water vapor. Measurements were taken at high frequency (20 Hz) and stored on a CR 5000 datalogger using a PCMCIA card. These measurements were collected and processed by an eddy-covariance software “ECpack” in order to derive sensible and latent heat fluxes by including all

corrections reported in Hoedjes et al. (2007 and 2008), Ezzahar et al. (2007b, 2009a , 2009b). For more information, table 1 summarizes the different meteorological and micro-meteorological instruments used in this study and their locations.

Imbalance in the closure of the energy balance with eddy-covariance system is a good measure of the quality of the convective fluxes data. To this objective, the sum of the latent (LE) and sensible (H) heat fluxes derived from the EC system was compared to the available energy (net radiation (R n) minus soil heat flux (G)) on both sites. For Agdal, the closure is very good with absolute values of average closure of about 8% and 9% of available energy during the 2003 and 2004 seasons, respectively (Hoedjes et al. 2008). For the R3 site, the absolute values of average closure were about 23% and 17% for 2002-2003 and 2012-2013 seasons, respectively. This is considered as acceptable with regards to literature (Twine et al., 2000).

Evapotranspiration partition

In addition to the EC observations, two techniques were used to measure separately the plant transpiration and the soil evaporation:

(1) Isotopes observations: The stable isotopes tracer technique was applied for the R3 site. This technique measures the isotopic compositions of Oxygen ($\delta^{18}O$) and Hydrogen ($\delta^{2}H$) of water fluxes from the soil water and foliage and quantifies the rate of the plant transpiration and soil evapotranspiration to the total evapotranspiration (ET). The sampling of soil, atmospheric and vegetation water samples were made during two days (Day Of Year -DOY- 101 and 102) of the growing season 2012-2013 and were analysed for their stable isotopic compositions of $\delta^{18}O$ and $\delta^{2}H$. It should be noted that the sampling was made during the development stage with cover fraction larger than 0.8. Also, the soil was very dry with a soil moisture of about 0.12 m^3/m^3 because the experiment was conducted before an irrigation event which was applied on DOY 104. Atmospheric water vapour was sampled from four heights (0cm, 85cm, 2m and 3m), between 10:00 and 16:00h with a frequency of 1hour on each sampling day. In addition, the samples of soil and vegetation were collected approximately between 13h and 14h. Afterwards, these samples were used to calculate $\delta^{2}H$ of the soil, vegetation and atmosphere in order to estimate the ET partition based on the Keeling plot approach and then to compare it with the modelled soil evaporation and plant transpiration. More details about the description of the principles and techniques of observations can be found in Aouade et al. (2016).

(2) Sapflow observations: Heat Ratio Method (HRM) was applied for Agdal site to measure xylem sap flux of eight olive trees using heat-pulse sensors. The period of measurement was situated between 9th of May (DOY 130) and the 28th of September (DOY 272) during 2004. This period is characterized by a hot climate with very high surface temperatures and thus presents a perfect period for studying the ET partition over such surfaces. In brief, this method uses temperature probes which were inserted into the active xylem at equal distances upstream and downstream from the heat source. This method was chosen due to its high precision at low sap velocities and its robust estimation of transpiration of olive (Fernandez et al., 2001). The heat-pulse sensors were equally inserted into large single and multi-stemmed trees located in the vicinity of the

EC tower. The transpiration at the field scale (in $mm.day^{-1}$) was obtained by scaling the measured volumetric sap flow ($L.day^{-1}$) based on a survey of the average ground area of each tree (45 m²). It is obtained by plotting the measured total evapotranspiration against the Sapflow observations under dry conditions leading to lower surface soil moisture when the soil evaporation is considered negligible (Williams et al., 2004; Er-Raki et al., 2010). This equation is then generalized for wet conditions of Sapflow observations for deriving the stand level plant transpiration. Finally, based on the EC observations, the obtained single tree transpiration was extrapolated to the EC footprint scale which is representative for the whole field (Er-Raki et al., 2010). Consequently, this can generate a significant error in estimating stand level plant transpiration as previously reported in several studies (Fernández et al., 2001; Williams et al., 2004; Oishi et al., 2008; Er-Raki et al., 2010).

Vegetation characteristics and irrigation inputs

For the Olive site, the mean vegetation fraction cover (F_c) and the leaf area index (LAI) obtained from one campaign of hemispherical canopy photographs (using a Nikon Coolpix 950 digital camera fitted with a fisheye lens converter 'FC-E8', field of view 183°) are equal to 55% and 3 m^2/m^2, respectively. For the wheat site, F_c and LAI together with vegetation height h_c were measured about every 15 days using the same instrument. Irrigation dates and amount were also gathered by dedicated surveys. Time series of LAI and reference evapotranspiration ET_0 are provided as supplementary material (Figure S1).

2.2 The ISBA-A-gs model description and implementation

2.2.1 Model description

ISBA is a land surface model used to simulate the heat, mass, momentum, and carbon exchanges between the continental surface (including vegetation and snow) and the atmosphere. It also prognoses temperature and moisture vertical profile in the soil. The first developed version of the ISBA model named thereafter as "standard version" based on a simple soil-vegetation composite scheme to compute the surface energy budget was developed by Noilhan and Planton (1989) and Noilhan and Mahfouf (1996). It is implemented within the open-access "Surface Externalisée" (SURFEX) platform version 8.1 developed at CNRM/Météo-France (Masson et al., 2013). In this study, a multilayer soil diffusion scheme (Decharme et al., 2011) is used to simulate the soil water and heat transfers instead of the initial force-restore formulation (Deardoff, 1977). The soil is vertically discretized by default into 14 soil layers up to 12 m depth to ensure a realistic description of the soil temperature profile (Decharme et al., 2013). Moisture and temperature of each layer is then computed according to their textural and hydrological characteristics. The latters (hydraulic conductivity and soil matrix potential) are derived from the Brooks and Corey (1966) parameterization following Decharme et al. (2013). The stomatal conductance and the photosynthesis are computed using the CO_2-responsive parameterization named A-g_s (Calvet et al., 1998, 2004). The model includes two plant responses to soil water stress functions depending on the plant strategy with regards to drought (Calvet,

2000; Calvet et al., 2004). Non-interactive vegetation option is chosen meaning that vegetation characteristics (LAI, height and fraction cover) are prescribed from *in situ* measurements with a 10-days time step. The multi-layer solar radiation transfer scheme (Carrer et al., 2013) which considers sunlit and shaded leaves is also activated. The root density profile is a combination of an homogeneous profile and of the Jackson et al. (1996) exponential profile (Garrigues et al., 2018). Full expressions of the aerodynamic resistances are given in Noilhan and Mahfouf (1996).

Compared to the standard version of ISBA-A-g_s, ISBA-MEB, for Multiple Energy Balance, solves up to three separated energy budgets for the soil and the snowpack following Choudhury and Monteith (1988). In this study, a double source arising from the soil and from the vegetation is used. For extended details about the different hypothesis used in MEB version as well as its full mathematical formulas and its related numerical resolution methods, the reader is referred to Boone et al. (2017). The main governing equations of both versions of the model are given in appendix 1.

2.2.2 Model implementation

Input parameters and data

ISBA within SURFEX is intended to be implemented using the patch approach where each grid point can include up to 19 patches representing 16 different plant functional type, bare soil, rock and permanent snow. Within the SURFEX platform, input parameters and variables are usually derived from the ECOCLIMAP II data base (Faroux et al., 2013). In this study, ECOCLIMAP II is bypassed by using *in situ* measurements for most of vegetation characteristics and albedo. For the wheat site, 10-days vegetation characteristics (LAI, h_c and F_c) were derived from *in situ* measurements based on a linear interpolation. Annual constant values were used for the Olive orchard. The roughness length for heat and momentum exchanges (Z_{0m} and Z_{0h}, respectively) are derived from h_c following Garratt (1992): $Z_{0m}=h_c/8$ and $Z_{0m}/Z_{0h}=7$. The emissivity and the total albedo are obtained as a linear combination of the soil and vegetation characteristics weighted by the fraction cover. The total albedo derived from the two components of the short wave net radiation measured by the net radiometer (CNR1) instruments are used to calibrate the albedos of vegetation and soil for the whole study field. The two component albedos remain constant for the whole set of simulations while the total albedo evolves through the vegetation cover fraction changes. Input data for the two sites are summarized in Table 2. Soil hydraulic properties were computed from the Clapp and Hornberger (Clapp and Hornberger, 1978) and the Cosby et al. (1984) pedotransfer functions. The resulting parameters were quite similar: $W_{wilt}=0.25$ and $W_{fc}=0.34$ for Clapp and Hornberger and $W_{wilt}=0.26$ and $W_{fc}=0.33$ for Cosby et al. (1984) Nevertheless, values obtained based on the calibration on soil moisture time series were quite different ($W_{wilt}=0.18$ and $W_{fc}=0.41$). Beyond the inherent uncertainties of the pedotransfer functions, this may be mostly explained by the lack of representativity of the soil sampling. Calibrated W_{wilt} and W_{fc} were imposed.

Model configurations

Three structural representations of the canopy are compared in this work: (1) the composite energy balance of the standard version named afterwards ″ISBA-1P″ for the single patch version; (2) the uncoupled version noted ″ISBA-2P″ for two patches, where the canopy and the soil patches are situated side-by-side, resolves two energy balance equations for both patches without any interactions concerning the turbulent heat exchanges. Likewise, the soil water dynamic is predicted on two uncoupled soil columns; (3) The coupled two layer approach of the new MEB version ″ISBA-MEB″ where the canopy layer is located above the soil component and the energy budgets of both layers are implicitly coupled with each other (Boone et al., 2017). Note that the ISBA-2P configuration is implemented on the Olive orchard only as there is no reason to represent the homogeneous canopy of wheat crops by two patches located side by side. Figure 2 displays the schematic representation of the 3 configurations of the model.

2.3 Sensitivity analysis and parameters calibration

2.3.1 Sensitivity analysis and calibration methods

Analyzing the sensitivity of the parameters one by one is not satisfactory because of the parameter interactions and non-linearities in the model equations and in the underlying processes (Pianosi et al., 2014). For this reason, the multi-objective generalized sensitivity analysis (MOGSA) (Goldberg, 1989; Demarty et al., 2005) is chosen in this study. The MOGSA methodology uses a Monte Carlo sampling of the search space. To represent the uncertainty of parameter estimates, an ensemble of N parameter set is drawn stochastically within a range of physically realistic values using an uniform distribution. A threshold on the targeted objective functions is then used to partition the ensemble into an “acceptable” and a “non-acceptable” regions. The trade-off between the targeted objectives is sought using a Pareto ranking scheme. The cumulative distribution of parameters value is compared to the normal distribution through the statistical Kolmogorov-Smirnorff (KS) test that relates this maximal distance to a probability value. The application of thresholds to this probability value permits to quantify the degree of parameter sensitivity. Ensemble of 20000 simulations for Agdal and 40000 for the R3 sites were computed. The size of simulations is related to the size of the studied period. Based on the recommendations of Demarty (2001), it is assumed that the size of the samples was large enough to obtain robust results. No account was taken of possible covariation between the parameter values in these prior choices of parameter sets because such covariation is generally difficult to assess. Several couple of objective functions was explored: latent heat LE and transpiration T_r, and sensible heat H and T_r, and LE/H. As similar sensitive parameters were highlighted, the chosen objective functions in this work were the convective fluxes H and LE. The MOGSA algorithm is also used to retrieve the parameter set providing the best trade-off of objective functions (Demarty et al., 2005). This parameter set will be called hereafter “optimal”. The ISBA model was thus calibrated by taking the best parameter set among the 20000 and the 40000 tested in the multi-objective sense. Finally, the validation step was carried out over the 2004 and 2013 seasons for Agdal and R3, respectively.

2.3.2 Sensitive parameters selection

For our sensitivity study, a total of 16 parameters (ϕ_v and ϕ'_v are for MEB only) were identified based on a previous knowledge of the model and the rich literature based on the use of ISBA-A-g_s and ISBA-MEB (Calvet et al., 2001, 2008; Boone et al., 1999, 2009, 2017; Napoly et al., 2017). The list of parameters and their ranges of variation are reported in Table 3. The land cover database obtained from ECOCLIMAP (Masson et al., 2003) and ECOCLIMAP-II (Faroux et al., 2013) were used to prescribe the range of variations of the input parameters. The same sensitivity analysis and calibration study were conducted for the standard single source version and the MEB version of ISBA. The sensitivity analysis was carried out for the whole 2003 wheat season for the R3 site and between 1st of June and 30 August (2003) over the olive orchard (Agdal site) in order to limit the computing time.

The parameters list includes : (1) some well known to be highly sensitive parameters such as the soil texture, the root depth and the ratio of roughness lengths Z_0/Z_{0H}; (2) some parameters of the A-g_s module: the mesophyllian conductance in unstressed conditions g_m, the maximum air saturation deficit $D_{\max}$, the cuticular conductance g_c and the critical normalized soil water content for stress parameterization θ_c (Calvet et al., 2000; Calvet et al., 2004; Rivalland et al., 2005); (3) the new parameters which were introduced in ISBA-MEB , such as the longwave radiation transmission factor, which determines the partition of this radiation between vegetation and soil (Boone et al., 2017) and the attenuation coefficient for momentum and for wind that prescribe changes based on canopy heights, turbulent transfer coefficients, and wind speed (Boone et al., 2017, Choudhury and Monteith, 1988). Values of these two parameters are, in the current version of ISBA, constant independently of the type of canopy (ϕ_v = 2 and ϕ'_v = 3) while Choudhury and Montheith (1988) have shown that this model is sensitive to the variation of those two parameters, in particular, the temperature of the ground surface, which depends, among other things, on the aerodynamic resistance between the source of movement at the vegetation level and the soil surface. Likewise, the aerodynamic resistance between the vegetation and the air at the vegetation level is related to ϕ'_v and to the Leaf width L_w (Choudhury and Monteith, 1988).

All parameters are common between the two versions except ϕ_v , ϕ'_v and L_w which concern the MEB version only.

3. Results

3.1 Sensitivity analysis and calibration

Only results of ISBA-MEB are presented here as quite similar list of sensitive parameters is obtained with the standard version of ISBA. The simulations are partitioned into two groups: "acceptable" and "unacceptable". Demarty et al. (2005) suggested that 7 to 10% of members should compose the “acceptable” set. In this context, 1720 acceptable simulations for the Agdal site (8.6%) and 3600 for the wheat site (9.0%) are retained. Figure 3 displays the results of the sensitivity analysis obtained for both sites. The horizontal dashed lines indicate the transition levels between ‘low’, ‘medium’ and ‘high’ sensitivity (Bastidas et al., 1999). Table 4 reports the optimal values of the highly sensitive parameters for at least one of the objective functions.

The high sensitivity of some parameters was anticipated such as: (1) the soil texture related parameters (fraction of sand and/or clay) that strongly impacts the hydrodynamic characteristics of the soil and, ultimately, the fluxes (Garrigues et al., 2015); (2) the root depth that has a major role in the extraction of available water in the root zone (Calvet et al., 2008); (3) the ratio of roughness lengths Z_0/Z_{0H}, which impacts the calculation of the aerodynamic resistance. Those parameters which highly affect the model behavior are usually estimated through *in situ* measurements or for a large-scale application from global data base. In both case, their values are uncertain, even at the station scale as their spatial variability remains significant, including the soil texture along the vertical profile. Five other sensitive parameters are also common to both sites in particular the long wave transmission factor τ_{LW} introduced in the new radiative transfer scheme and the parameters introduced in the ISBA-MEB version L_w, ϕ_v, ϕ'_v and U_l. Concerning the attenuation coefficient of the movement ϕ_v, Choudhury and Montheith (1988) had already shown the strong sensitivity of the model to this parameter especially for dry soils encountered in our study sites.

Concerning the Agdal site, results showed 11 sensitive parameters, 8 parameters with ‘high’ sensitivity and 3 with ‘medium’ sensitivity (Figure 3a) when at least one of the objective functions are considered. The chosen period was characterized by a gradual drying of the soil with a water stress detected on day 190 (Ezzahar et al., 2007a). The plant transpiration thus represented the main component of the evapotranspiration. Within this context, the identified sensitivity of parameters directly impacting the stomatal regulation (g_m, $D_{\max}$) and the availability of water in the soil (Sand, Clay and RD) is consistent. Regarding the moderate fraction cover (F_c=0.55) and the flooding technic applied for irrigation, soil evaporation tightly related to soil texture as well may not be negligible on the site. Interestingly enough, the obtained optimal values of 0.47 for Sand and 0.27 for Clay (Table 4) were very close to the *in situ* measurements. The root depth (RD) influences also strongly convective fluxes. An optimal value of 0.62m. was found while literature as well as ECOCLIMAP, propose deeper rooting depth up to 1.5m. for perennial trees. Nevertheless, it is well known that roots develop in the upper wet layer of the

soil when irrigation is applied (Fernandez et al., 1990) while deeper development can be observed in case of water supply problems only (Maillard, 1975). Additionally, the soil in our site below 1 m. is very compact and contains rocks which limit the development of the pivoting roots.

For the wheat site, the sensitivity analysis revealed 13 sensitive parameters: 8 of them have a 'high' sensitivity and 5 of them with a 'medium' sensitivity (Figure 3b). As for the Agdal site, specific parameters are related to the soil (like Cl) and others related to the crop (RD, L_w and τ_{LW}). By contrast to Agdal, the two fluxes LE and H showed also a strong sensitivity to the Z_0/Z_{0H} parameter. In the standard version of ISBA-A-g_s, this ratio is equal to 10 according to Braud et al. (1995) and Giordani et al. (1996), but at the station scale, several studies have shown that this ratio could range from 1 to 100 (Napoly et al., 2017). The optimal value for the wheat site was 7.00. The obtained optimal lower value increases the amplitude of H and reduces that of the surface temperature. This is consistent with similar findings of Beziat et al. (2013) for a wheat site located in the South-West of France. Literature as well as ECOCLIMAP, propose values of root depths of about 0.50 m for our type of crop (Crop C3). In our case, a slightly higher value of 0.55 m appeared optimal for latent heat fluxes and also for transpiration when compared to the isotopic measurements (see comments below and Table 4). This is an acceptable value for irrigated wheat in the region (Duchemin et al., 2006, Er-Raki et al., 2007). Due to the limited number of irrigations on this site, the plant tends to extend roots to deeper layers to extract water. The slightly lower value of clay content (0.44) than the *in situ* measurement (0.47) adjustment is also consistent by limiting water retention and favors water availability in the deepest layers. Regarding the evapotranspiration flux, in the case of a dry soil, the only possible solution to reproduce the experimental data is to increase transpiration of the crop. Indeed, the strong sensitivity of the two parameters ϕ_v and ϕ'_v, seems to be consistent (Choudhury and Idso 1985). In addition, the optimal value for ϕ_v (ϕ'_v) is higher (lower) than literature (Table 4).

As a conclusion, the optimal values of the sensitive parameters being significantly different from literature values, studies at the local scales should be duplicated to determine specific parameters values for different eco- and agro-systems in the view of a large-scale applications.

3.2 Composite energy budget

3.2.1 Latent heat flux

Figure 4 displays the daily time series of latent heat fluxes using the three configurations of the ISBA model for both sites. The irrigation and rainfall events are also superimposed. Please note that hereafter daily values refer to average of diurnal values between 9h and 17h local time. The same figure but for the sensible heat flux is provided as supplementary material (Figure S2). Statistical metrics for the four components of the energy budget are reported in Table 5. The seasonal dynamic of LE is properly reproduced by the model for both sites whatever the configuration. ISBA-2P and ISBA-MEB definitely

outperformed the ISBA-1P version on average over the olive orchard for both seasons with RMSE values below 52.2 W/m², while for ISBA-1P, RMSE can reach up to 107.1 W/m². This corresponds to average errors of 19% and 16% for MEB in 2003 and 2004, respectively; 28% and 21% for ISBA-2P while average error is about 42% for ISBA-1P during both years. By contrast, over the wheat site, the ISBA-1P version is much closer to ISBA-MEB with differences of RMSE around 10 W/m². Average errors are also closed: 23% versus 21% for MEB and ISBA-1P in 2003 and 26% versus 28% in 2013. This means that:

(1) the dual source configurations are better suited to predict composite LE for row crops of moderate fraction. This results is in line with Napoly et al. (2017: Fig. 15b), ISBA-1P and ISBA-MEB differences (biggest improvements for MEB) are largest for LAI values in the range from 3 to 4 m2/m2 corresponding to moderate Fc, which corresponds to the LAI for the olive grove in this study. This arises mainly because the differences between the surface and the vegetation (temperatures, fluxes…) are most contrasted for sparse vegetation cover. By contrast, when Fc tends to 1, ISBA-1P resembles a completely vegetation surface and ISBA-MEB and ISBA-1P should converge.

(2) in contrast as expected, a simple composite energy budget can cope with the homogeneity of the wheat canopy at least to predict LE. Generally speaking, the difference between ISBA-1P and ISBA-MEB in terms of surface temperatures, fluxes, etc. is expected to decrease as the cover decreases in height: the results converge as the surface becomes devoid of vegetation. So, results tend to be closer for grasses and annuals just like wheat than trees. This is because the main differences arise owing to the difference in the within-canopy turbulence treatment: both versions use the same functions based on MOST above the momentum sink point (z0 for ISBA-1P, z0+d for ISBA-MEB where d is the displacement height) meaning that as the $d \rightarrow 0$, the models converge to a certain extent. Likewise, when Fc becomes tends to 1, ISBA-1P resembles a completely vegetated surface and ISBA-MEB and ISBA-1P converge. The added value of a double energy budget should thus be evident from emergence until full cover when vegetation is sparse. The surface can be considered homogeneous out of this period either considering bare soil at the start of the season or fully covering vegetation after. By contrast, from emergence to full cover, the cover sparsity may lead to a strong difference between soil and vegetation temperatures and some level of coupling between both energy sources but this period is short for wheat. It covers less than 1 month around march at +/- 10 days.

(3) The slightly better results obtained with ISBA-MEB than with ISBA-2P on the Olive orchard demonstrates that the soil and the vegetation heat sources are coupled to some extent. This is probably because the bare soil area between the tree rows (the inter-row is about 8 m) is not sufficiently large to consider that soil and vegetation heat sources doesn't interact with each other by locating the two sources side by side.

Previous studies have already demonstrated the limit of single source models for predicting surface fluxes over sparse vegetation. Jiménez et al. (2011) have evaluated four single source (Mosaic, Noah, Community Land Model -CLM-, and Variable Infiltration Capacity -VIC-) at the global scale and they showed their limitations for producing latent and sensible heat fluxes over tall and sparse vegetation such as forest canopies. Likewise, Blyth et al. (1999) over Sahel estimated more accurately the surface fluxes over Savannah with the dual source version of the MOSES model compared to the original single source version. Our results with the new ISBA-MEB version implemented within the SURFEX platform are consistent with these previous findings.

Another interesting feature is the observed departure between model predictions and observations around irrigation events. Nevertheless, the different configurations of the model strongly differ during these specific periods, in particular over the Olive site. In line with the observations, the three configurations show a strong shift of the available energy from sensible to latent heat when irrigation occurs (see also sensible heat flux time series, figure S2) but, while this shift is moderate and in overall agreement with the observations for the dual source configurations, it is strongly emphasized by ISBA-1P. For instance, LE predictions reached a maximum of about 550 W/m² in mid-June for both seasons 2003 and 2004, observations remained below 400 W/m². To a lesser extent, this trend to unreasonable shifting also occurred for the ISBA-2P especially when the available energy is very high (during the summer months of the 2003 season). The reverse behavior is obviously observed for H (Figure S2): after each irrigation event, the simulated sensible heat by ISBA-1P dropped considerably due to the drastic decline in simulated surface temperature by this version. In addition to the model deficiencies at the time of irrigation as already highlighted, part of the discrepancies between simulations and observations can be related to the eddy eddy-covariance measurements because of the associated strong heterogeneity within the footprint during an irrigation event.

In contrast, on the wheat site, the dynamics of the latent heat flux is smoother than at the Olive site in 2013 and, to a lesser extent in 2003, in particular because of a persistent cloud cover during the first two weeks of March (see the drastic drop of ET_0, Figure S1). The year 2003 is also characterized by lower LE values mainly because several successive drought years in the beginning of the 2000s cause a drop of dam levels and limited the water availability for irrigation. Indeed, the total cumulated rainfall and irrigation was 351mm for the 2002-2003 season while it reached about 770mm for 2012-2013. By contrast to the Olive site, the two configuration of the model are able to reproduce the overall seasonal dynamic of LE for these two contrasted years. The only exception is around the late season irrigation events in April and May for year 2013 during which ISBA-1P showed the same trend to strongly emphasize the energy shift as already highlighted for the Olive site.

As a conclusion, while dual sources configuration outperformed the single source version of the model for the complex and sparse Olive canopy, a composite single energy budget is able to reproduce the seasonal dynamic of LE for the homogenous wheat cover. At this level of sparsity for the Olive orchard, the coupling between soil and vegetation heat source is moderate as both the patch uncoupled and the coupled layer configurations provided close statistical metrics. For the Olive site,

significant drawback of ISBA-1P and, to a lesser extent, ISBA-2P is highlighted during the strong transient regime associated to the irrigation events.

3.2.2 Other components of the energy budget

The performance of the different configurations to simulate the other components of the energy budget R_n, H and G was investigated using a Taylor diagram (Figure 5). This presentation summarizes graphically the comparison between the model and the observations based on the root mean square difference, the correlation coefficient r and the standard deviations (Taylor, 2001). Statistical metrics are reported in Table 5.

The net radiation is almost perfectly simulated by the three configurations with slight differences related to the budget in the longwave. Values of the albedo are identical for the three configurations and have been calibrated on the short wave components of R_n measured by CNR1. For both sites, the correlation coefficient r is close to 1.0 and the RMSE is lower than 25.0 W/m². These good performances are in agreement with results reported in the literature. Indeed, several studies showed that the estimation of R_n by SVAT models is good on several type of canopy (Napoly et al., 2017, Boulet et al., 2015, Ezzahar et al., 2007a and 2009a). The most important differences are encountered on the Agdal site and can be explained by the slight overestimation (not shown) of the infrared radiation (LW_{up}) by ISBA-2P for both seasons (Bias=13.7 and 12.7 W/m^2 for the 2003 and 2004 seasons, respectively). For this configuration, the soil of the soil patch directly exposed to the solar radiation becomes very hot and dissipates much less energy by soil conduction compared to the other two configurations. This is due to a compensation between the soil and the vegetation patches as explained below.

For the sensible heat fluxes (figure S2), the dual sources configurations ISBA-2P and ISBA-MEB also outperformed the single source version ISBA-1P for sensible heat flux predictions over the olive orchard. In contrast, the two tested configurations are much closer for the wheat site with RMSE of 55.2 and 55.0 W/m^2 in 2003 for ISBA-1P and ISBA-MEB, respectively. The temporal dynamics is also greatly improved since the correlation coefficients (r) are above 0.8 for the dual source configurations for the 2 seasons at the olive orchard site whereas they are only of 0.7 and 0.6 for the simple source approach. Here again, it is the shifting between sensible and latent heat fluxes during the irrigation events and during the drying period that leads to the differences between single and dual sources configurations. For the wheat site, the behaviors are very similar for the two configurations although the MEB version presents the best performances.

Due to the complexity of the canopy surface and the spatial variability of the hydric and thermal conditions, particularly because of the shading effects, the ground heat flux is the most difficult component of the energy budget both to simulate and to measure. The heat plates fluxes used on both studied sites have a very low representativeness which does not exceed a few tens of centimeters whereas the illumination can be very variable under a relatively open canopy such as olive or over wheat at the beginning of the season. Therefore, the obtained results should be interpreted with caution. The highlighted improvement on the turbulent fluxes using –MEB with regards to the two other configurations is not so clear for the

conduction fluxes. It seems that MEB has a systematic tendency to dissipate too much energy by conduction (see biases on Table 5). On average on the two years for the Olive site, the ISBA-2P configuration has the best overall performance in predicting G. Nevertheless, by taking a closer look on the daily cycles of the ground heat flux with a distinction between the bare soil patch and the vegetation patch (see figure S3), it appears that the patch bare soil dissipates much more energy by conduction than ISBA-MEB as shown by the amplitude of the daily cycles which is much stronger than observations. By contrast, the patch vegetation (LAI =5 and a cover fraction close to 1) dissipates less energy by conduction in favor of the convective fluxes. The average ground heat flux (derived as the sum of the two components weighted by their respective fraction cover) is in good agreement with observations even if none of the 2 patches represent correctly the observed fluxes. This tends to show that the uncoupled approach is quite suitable for predicting total G over this sparse and relatively open cover but for the "wrong" reasons. Finally, ISBA-1P also dissipates much more energy than ISBA-MEB because soil experience little shading as explained below (see 3.1.1).

3.3 Soil and Vegetation components

In this section, soil and vegetation components of the radiation budget and of the partition of evapotranspiration were analysed. Please note that only the olive orchard site was considered for the radiation budget components as the experimental design on the wheat site could not sample each component separately. For ISBA-2P, vegetation and soil refers to the components predictions of the respective patches while for ISBA-1P, the soil-vegetation composite variables are plotted.

3.1.1 Radiation budget

Figure 6a displays the time series of the soil net radiation simulated by the three configurations at the Agdal site in 2003 season. Similar conclusions can be drawn from the data acquired in 2004. The ''bare soil'' patch is shown for the ISBA-2P configuration. The amplitude of the seasonal cycle is much stronger for the observations than for the ISBA simulations. The net radiation at the soil surface is obviously lower for ISBA-MEB because of the vegetation screening and a real partition between the two sources than for ISBA-1P and -2P (soil patch). Indeed, for ISBA-1P, there is no partition of net radiation between soil and vegetation. Stated differently, since with only one energy budget, soil temperature is the same as the temperature of the vegetation, soil experience very little shading (in addition, it uses the same -relatively large- z0 since the nonlinear aggregation of z0 for soil and vegetation tends to result in a z0 much closer to the higher elements -the vegetation z0-, as one would expect). The high available energy (Figure 6) is used for soil evaporation at the time of irrigation (see Figure S4) unless Fc→1. ISBA-MEB is in better agreement with observations during the winter months while the agreement is better in summer for ISBA-2P and ISBA-1P. The strong differences may also be related to observations. Indeed, the soil net radiation was measured under cover. When the cover is sparse, as for the olive trees, it is very difficult to screen it totally from direct incoming radiation as during summer, with a solar zenith angle close to 0, the instrument is exposed to direct radiation. In winter, ISBA-MEB appears to be well reproducing the measurements of the available energy at the ground-level when the instrument may be shadowed by the canopy. When the instrument is exposed to direct

illumination, the ISBA-1P configuration and the bare-soil patch of the ISBA-2P configuration are obviously closer to observations.

Figure 6b displays the time series of the soil temperature at the Agdal site in 2003. The new coupled version limits the available energy arriving at the ground level compared to ISBA-1P and therefore leads to the lower predicted temperatures. The patch bare soil of the ISBA-2P configuration exhibits the higher values of soil temperature because it is directly exposed to incoming solar radiation. On average, biases for ISBA-MEB and ISBA-1P are moderate but it is due to an overestimation by both configurations during winter while an underestimation is observed during summer. Indeed, for the winter months, the temperature sensor observes mainly areas of shaded bare ground while, during summer, the observed soil is under the influence of direct illumination. At this time, the bare soil patch of the ISBA-2P configuration presents the best agreement with the observations (Bias= -2.3° for June to September compared to -6.6° and -6.7° for ISBA-1P and ISBA-MEB, respectively). Moreover, this negative bias is mainly attributed to the few days following the irrigation events for which the bare soil patch simulates a much greater cooling. The difference reaches more than 7.0°, three days after the irrigation at the beginning of August in particular. On the other hand, when the soil is dry (more than 10 days after each irrigation), the difference is less than 1.5°. There is also a fairly clear over-estimation during the winter months. At this time of the year, H is slightly underestimated.

Finally, figure 6c is the same as figure 6b but for vegetation temperature. These observations may be more reliable than the observations of the soil temperature even if some parts of the bare soil can disturb the representativeness of the observations. The three configurations are much closer than for the observations of soil temperature and reproduce reasonably well the observations with RMSEs of 4.5°, 4.6° and 4.2° for ISBA-1P, ISBA-2P and ISBA-MEB, respectively. A large part of these errors can be attributed to the positive bias of the three configurations. The ISBA-MEB version has the lowest bias while the ISBA-1P and ISBA-2P versions are logically slightly warmer. Indeed, ISBA-MEB is able to partition the energy between the soil and vegetation components whereas the two other configurations simulate a composite temperature resulting from the resolution of a composite energy balance with a hot surface layer most of the year.

3.3.2 Partition evaporation/transpiration

The plant transpiration measured by the Sapflow method and the stable isotopic technique is compared to those simulated by ISBA during the 2004 and 2013 seasons for the olive and wheat sites, respectively. The transpiration measured by the Sapflow at the Olive orchard site was aggregated at a daily timescale and converted in mm/day. Concerning the isotopic measurements at the wheat site, it was given as the ratio of the total evapotranspiration flux. It is important to state that only the coupled version of ISBA-MEB is able to provide a partition the total evapotranspiration in a bio-physically based manner. Indeed, the single source version of ISBA used in the ISBA-1P and in the ISBA-2P configurations partitions artificially the evapotranspiration based on the cover fraction (Noilhan et Planton, 1989). Table displays the average

percentage of transpiration predicted by ISBA-1P and ISBA-MEB and measured by the stable isotope method during the two days of sampling over the wheat site. As expected, the results show that the two configurations give increasing values which are in good accordance with the dynamic of the drying-out of the bare soil. By contrast, values of measured transpiration show an inverse dynamic. This is mainly attributed to the sampling areas which were characterized by a higher percentage of the bare soil for the first day compared to the second one. The problem of the sampling representativeness by the stable isotope method has been detailed in Aouade et al. (2016) using the same data. An average value of the two days was used for comparison in order to improve the observations representativeness. The two configurations show that the transpiration dominates ET and ISBA-1P and ISBA-MEB values are fairly close to the observations in spite of a light underestimation (overestimation) of ISBA-1P (ISBA-MEB).

Figure 7 presents the time series of the plant transpiration simulated by the three configurations and measured by the Sapflow method during the 2004 summer season at the Agdal site. ISBA-MEB outperformed the two other configurations based on the single source version with an RMSE of 0.7 mm/day, a correlation coefficient r=0.73 and a small bias. ISBA-2P predictions are also quite good but with a moderate underestimation of 1 mm/day. By contrast with the dual-sources configurations, the result of the ISBA-1P is significantly worst with an RMSE of about 1.7 mm/day, a low value of r = 0.4 and a strong negative bias of about -1.5 mm/day. Although ISBA-1P and 2-P significantly overestimated the total ET after an irrigation events compared to ISBA-MEB, they underestimated largely the transpiration. This underestimation of ISBA-2P and -1P is in agreement with the higher available energy and, in fine, soil evaporation of these two configurations with regards to ISBA-MEB (see time series of predicted soil evaporation as supplementary material; Figure S4). For ISBA-2P, this is because (1) the large soil patch is directly exposed to the incoming solar radiation with no vegetation screening and (2) there are obviously no roots to extract water on this patch. Indeed, the evaporation flux for ISBA-2P is of the same order of magnitude as the 1P configuration but because of a strong contrast between the patch "bare soil″ that dominates the total evaporation while the “vegetation” patch evaporation is very low (Figure S4). ISBA-MEB represents also a peak of evaporation after each irrigation event but stills much more moderate than for the other two configurations. This is due to the lower available energy at the ground level than for the other configurations already highlighted. For ISBA-1P, a large part of this energy is also dissipated by conduction, as was already explained. Finally, the drastic drop of predicted transpiration by ISBA-2P and, to a lesser extent, by ISBA-MEB around mid-august, is probably related to the ability of the olive trees to reach deeper soil layer where water is available while a constant rooting-depth is used in the model. Nevertheless, it is important to keep in mind that the scaling up of Sapflow data from a set of sample trees to the entire plot is a complex processes that relies on an empirical equation. As a conclusion, although no direct soil evaporation measurements were available, the overall good agreement of ISBA-MEB with transpiration measurements, in particular its small bias, tends to prove that it significantly improves the evapotranspiration partition with regards to the single composite energy budget of ISBA-A-gs in the case of tree cover of moderate sparsity.

3.4 Soil hydric budget

A comparison between simulated and observed soil moisture at Agdal and R3 sites is presented in this section. Soil moisture measurements are available at a half-hourly time steps at the surface layer (5cm) at Agdal site for 2003 season and at 5 and 60cm at the R3 site for the 2003 season.

Figure 8 displays the measured and simulated superficial soil moisture for the wheat and olive sites during the 2003 season and the soil water content in the root zone for the wheat site only. The three configurations show a good agreement with measurements, with moderate RMSE and Bias. However, ISBA-1P tends to dry out the surface layer too fast after each irrigation event, except during the summer month, which support a too high evaporation as already mentioned. This trend to to emphasize evaporation makes the statistical metrics of the single-source configuration slightly worse than the two dual-sources configurations. Interestingly, ISBA-2P and ISBA-MEB provides close prediction of surface soil moisture but, as already highlighted, this is because the high evaporation of the bare soil patch is compensated by the low evaporation of vegetation patch representing a close canopy. During the summer (high evaporative demand), the soil moisture falls to the residual value for ISBA-2P and ISBA-MEB during the severe drought on summer months, due mainly to the deficiency of irrigation between mid-June and August.

4. Discussion and conclusion

The present study was carried out in order to evaluate the ability of the multi energy balance version (MEB) of the Interactions Soil-Biosphere-Atmosphere land surface model (ISBA) to simulate the total energy fluxes and its vegetation and soil components including evapotranspiration (ET) and its partition into soil evaporation (E) and plant transpiration (T_r) for irrigated crops in semi-arid areas. Two dominating crops of the South Mediterranean region are chosen: an olive orchard and a winter wheat site located in Tensift Al Haouz (Center of Morocco). Observations of ET with an eddy-covariance systems and of T_r with Sapflow and Isotopic technics were used to validate the performance of ISBA-MEB (coupled scheme) compared to two other configurations of ISBA: 1 patch which is the classic big leaf approach (ISBA-1P) and 2 patches which corresponds to a two adjacent component approach (ISBA-2P) or uncoupled scheme.

The contrast of canopy geometries between the two crops leads to significant differences of behavior between the three configurations of the model:

- For an homogeneous cover like wheat, the ability of all the configurations to reproduce the composite soil-vegetation heat fluxes is very close. For the latent heat flux for example, the differences between RMSEs of ISBA-1P and -MEB are about 10 W/m² (corresponding to average errors differences lower than 4%). These results are consistent with many studies showing that the use of a composite energy balance on homogeneous cover crops is sufficient to provide a good reproduction of convective fluxes (Vogel et al., 1995, Noilhan and Mahfouf 1996). For the olive orchard which represents an open canopy (fraction cover of 0.55), both dual-sources configurations outperformed the single-source version.
- An analysis of the components of the uncoupled approach (ISBA-2P) shows a strong compensation between fluxes of the bare soil and the vegetation patches for the olive orchard. For instance, evapotranspiration after each irrigation event is strongly overestimated mainly due to strong soil evaporation. This is attributed to a large available energy at the surface directly exposed to incoming radiation coupled to an absence of root extraction for the bare soil patch. Stated differently, the aggregated flux is close to the coupled version (ISBA-MEB) and to the observations but for the "wrong" reasons.

In addition, another specificity of our study focused on irrigated crops in semi-arid areas is the strong transient regime around an irrigation event leading to a strong shift of energy between sensible and latent heat fluxes. The consequence of the differences of surface representation between the three model configurations (root distribution, available energy, heat source coupling …) lead to exacerbated consequences on the energy budget components at this time. Figure 9 summarizes the behavior of the three configurations around an irrigation event for the Olive orchard. It displays the average time series of predicted and observed surface temperature (T_s), ground heat flux (G), and the convective heat fluxes (H and LE) from 5 days before to 8 days after an irrigation event. Irrigation causes obviously a drop of the composite soil/vegetation

temperature (Figure 9a). The energy is therefore mainly attributed to the latent heat flux (Figure d) at the expense of the sensible heat flux (Figure 9c). This is predicted by the three configurations of the model but with different level of accuracy. The differences of the configuration behaviors at this time explain, to a large extent, the differences in the overall performance between the simple balance configuration and the two others. ISBA-1P shows abnormally high values of LE after an irrigation event. By contrast, ISBA-2P and above all, ISBA-MEB are able to better reproduce the observed moderate shifting.

One of the main conclusions of the study is that the new ISBA-MEB version implemented in the SURFEX platform has proved to be more suitable than single source configuration for estimating turbulent fluxes including evapotranspiration and its components, at least for moderately open tree canopies. This shows the need to take into account the interaction between vegetation and soil acting as coupled sources of heat in the parameterization of SVATs when vegetation is sparse. The choice between coupled and uncoupled model, to better represent exchanges between the biosphere and the atmosphere, is not straightforward anyway. The obtained results demonstrated that the coupled energy balance provided also the best estimates of components and composite fluxes but the patch approach followed closely. Likewise, this study also showed, as suggested by Choudhury and Monteith (1988), that the new parameters introduced in ISBA-MEB (such as the attenuation coefficient for momentum and for wind) are highly sensitive and vegetation-type dependent as evidenced by the different calibrated values between the two studied crops. This study points out the need for further local scale evaluation on different crops of various geometry (more open rainfed or denser intensive olive orchard) and over different climatic conditions in order to assess in particular from which degree of sparsity, a dual source approach should be preferred. This will both further our understanding of the representation of soil and vegetation heat sources in the SURFEX platform and also help to provide adequate parameterization to global data base such as ECOCLIMAP-II in the view of a global application of the ISBA-MEB model. Finally, considering the heavy trend towards the conversion of traditional (wheat) crops to tree crops in the south Mediterranean region, which are more financially attractive but that also consume more water (Jarlan et al., 2015), improving the representation of complex crops in SVAT model is also of prime importance for future studies on surface-atmosphere retro-action or global change impact.

Code and data availability

The MEB code is a part of the ISBA LSM and is available as open source via the surface modeling platform called SURFEX, which can be downloaded at http://www.cnrm-game-meteo.fr/surfex/. Validation data on both sites may be distributed on request to the co-leads of the Tensift observatory Pr. Jamal Ezzahar (j.ezzahar@uca.ma) and Dr. Vincent Simonneaux (vincent.simonneaux@ird.fr)

Acknowledgements

This work has been carried out within the frame of the Joint International TREMA (IRD, UCAM, DMN, CNESTEN, ABHT, ORMVAH) and of the ERANETMED03-62 CHAAMS project. Financial supports for the experiment have been provided by IRD, the MISTRALS/SICMED program through the METASIM project, the ANR AMETHYST project (ANR-12-TMED-0006-01), the SAGESSE project (Projet Prioritaire de Recherche PPR - Type B), funded by the Minister for Higher Education, Scientific Research and Executive Training (Morocco), PHC Toubkal TBK/18/61, the H2020 PRIMA ALTOS project and the RISE REC project (H2020/645642) financed by the Marie Skłodowska-Curie Research and Innovation Staff Exchange (RISE). G. Aouade received a travel grant from the MISTRALS/ENVIMED program through the CHAMO project and a financial support from MISTRALS/SICMED2.

Author contributions

Aouade G., Jarlan L., worked out almost all of the technical details, performed the numerical calculations for the suggested experiment and took the lead in writing the manuscript. Jarlan L., Ezzahar J. and Boone A., conceived the original idea and supervised the findings of this work. Er-raki S., Benkaddour A., Khabba S., Boulet G., Garrigues S., Chehbouni A., Boone A., Napoly A., contributed to the interpretation of the results and to the final version of the manuscript. Boone A., Napoly A., designed the model and the computational framework. All authors provided critical feedback and helped shape the research, analysis and manuscript.

References

Allen, R.G., Pereira, L.S., Raes, D., Smith, M.: Crop Evapotranspiration-Guidelines for Computing Crop Water Requirements, Irrigation and Drain, Paper No. 56. FAO, Rome, Italy. 300, 1998.

Aouade, G., Ezzahar, J., Amenzou, N., Er-Raki, S., Benkaddour, A., Khabba, S., Jarlan, L.: Combining stable isotopes and micrometeorological measurements for partitioning evapotranspiration of winter wheat into soil evaporation and plant transpiration in a semi-arid region. Agric. Water Manag. 177, 181–192, 2016.

Avissar, R. and Pielke, R.A.: A parameterization of heterogeneous land surfaces for atmospheric numerical models and its impact on regional meteorology. Mon. Wea. Rev. 117: 21 13-2136, 1989.

Bastidas, L. A., Gupta, H. V., Sorooshian, S, Shuttleworth, W. J. and Yang, Z. L.: Sensitivity analysis of a land surface scheme using multicriteria methods. J. Geophys. Res., 104, 19481 – 19490, 1999.

Béziat, P., Rivalland, V., Tallec, T., Jarosz, N., Boulet, G., Gentine, P., Ceschia, E.: Evaluation of a simple approach for crop evapotranspiration partitioning and analysis of the water budget distribution for several crop species. Agricultural and Forest Meteorology, 177, 46-56, 2013.

Blyth E.M.,Harding R.J., and Essery R.: A coupled dual source GCM SVAT. Hydrology and Earth system Sciences, 3(1), 71-84, 1999.

Blyth, E.M. and Harding, R.J.: Application of aggregation models to surface heat flux from the Sahelian tiger bush. Agric. For. Meteorol., 72 , 213-235, 1995.

Bonan GB, Williams M, Fisher RA, Oleson KW.: Modeling stomatal conductance in the earth system: linking leaf water-use efficiency and water transport along the soil-plant-atmosphere continuum. Geosci Model Dev 7: 2193–2222, 1995.

Boone, A., Calvet, J., and Noilhan, J.: Inclusion of a third soil layer in a land surface scheme using the force-restore method. Journal of Applied Meteorology, 38,1611–1630, 1999.

Boone, A., De Rosnay, P., Balsamo, G., Beljaars, A., Chopin, F., Decharme, B., Delire, C., Ducharne, A., Gascoin, S., Grippa, M.: The amma land surface model intercomparison project (almip).Bulletin of the American Meteorological Society, 90(12), 1865-1880, 2009.

Boone, A., Samuelsson, P., Gollvik, S., Napoly, A., Jarlan, L., Brun, E., & Decharme, B.: The interactions between soil-biosphere-atmosphere land surface model with a multi-energy balance (ISBA-MEB) option in SURFEXv8-Part 1: Model description. *Geosci. Model Dev.*, *10*(2), 843-872, 2017.

Boone, A., Masson, V., Meyers, T., and Noilhan, J.: The influence of the inclusion of soil freezing on simulations by a soil-vegetation-atmosphere transfer scheme. J. Appl.Meteor., 9, 1544–1569, 2000.

Boulet G, Mougenot B, Lhomme J.-P, Fanise P, Lili-Chabaane Z, Olioso A., Bahir M. , Rivalland V., Jarlan L., Merlin O., Coudert B., Er-Raki S. and Lagouarde J.-P.: The SPARSE model for the prediction of water stress and evapotranspiration components from thermal infra-red data and its evaluation over irrigated and rainfed wheat. Hydrology and Earth System Sciences, 19, 4653-4672, 2015.

Boulet G., Chehbouni A., Braud I., Vauclin M.: Mosaic versus dual source approaches for modelling the surface energy balance of a semi-arid land. Hydrology and Earth System Sciences,3 (2), 247-258, 1999.

Braud,I, Dantas-Antonino, AC, Vauclin, M, Thony, J.L. and Ruelle, P.: A simple soil-plant-atmosphere transfer model (SiSPAT) development and field verification. Journal of Hydrology, 166(3-4), 213-250, 1995.

Brooks, R. H., and A. T. Corey.: Properties of porous media affecting fluid flow, J. Irrig. Drain. Am. Soc. Civil Eng. 17, 187-208., 1966.

Burgess, S.S.O., Adams, M.A., Turner, N.C., Beverly, C.R., Ong, C.K., Khan, A.A.H., Bleby, T.M.: An improved heat pulse method to measure slow and reverse flow in woody plants. Tree Physiology. 21, 589-598, 2001.

Burke, E.J., Gurney, R.J., Simmonds, L.P., Jackson, T.J.: Calibrating a soil water and energy budget model with remotely sensed data to obtain quantitative information about the soil. Water Resources Research 33, 1689–1697, 1997.

Calvet, J. C. and Soussana, J.-F.: Modelling CO_2-enrichment effects using an interactive vegetation SVAT scheme. Agr. For.Meteorol., 108, 129–152, 2001.

Calvet, J.C. Investigating soil and atmospheric plant water stress using physiological and micrometeorological data. Agricultural and Forest Meteorology, 103(3), 229–247, 2000.

Calvet, J.-C., Gibelin, A.-L., Roujean, J.-L., Martin, E., Moigne, P. L., Douville, H., and Noilhan, J.: Past and future scenarios of the effect of carbon dioxide on plant growth and transpiration for three vegetation types of southwestern France. Atmospheric Chemistry and Physics, 8(2), 397–406, 2008.

Calvet, J.-C., Noilhan, J., Roujean, J.-L., Bessemoulin, P., Cabelguenne, M., Olioso, A., and Wigneron, J.-P.: An interactive vegetation svat model tested against data from six contrasting sites. Agr. For. Meteorol., 92:73–95, 1998.

Calvet, J.-C., Rivalland, V., Picon-Cochard,C., Guehl, J.-M.: Modelling forest transpiration and CO_2 fluxes - response to soil moisture stress, Agric. For. Meteorol., 124(3-4), 143-156, doi: 10.1016/j.agrformet.2004.01.007, 2004.

Canadell, J., Jackson, R.B., Ehleringer, J.B., Mooney, H.A., Sala, O.E., Schulze, E.D.: Maximum rooting depth of vegetation types at the global scale, Oecologia, 108, 583-595, 1996.

Carrer, D., Roujean, J.-L., Lafont, S., Calvet, J.-C., Boone, A., Decharme, B., Delire, C.and Gastellu-Etchegorry, J.-P.: A canopy radiative transfer scheme with explicit fapar for the interactive vegetation model isba-a-gs: Impact on carbon fluxes. Journal of Geophysical Research, 118(2), 888–903, 2013.

Cermák J., Deml M., Penka M.: A new method of sap flow rate determination in trees. Biol. Plant 15, 171–17810.1007/BF02922390, 1973.

Cermák J., Kucera J., Nadezhdina N.: Sap flow measurements with some thermodynamic methods, flow integration within trees and scaling up from sample trees to entire forest stands. Trees (Berl. West) 18, 529–54610.1007/s00468-004-0339-6, 2004.

Chehbouni ,A., Escadafal ,R., Duchemin ,B., Boulet, G., Simonneaux ,V., Dedieu, G., Mougenot, B., Khabba, S., Kharrou ,H., Maisongrande, P., Merlin ,O., Chaponnière, A., Ezzahar, J., Er-Raki ,S., Hoedjes, J., Hadria, R., Abourida, A., Cheggour, A., Raibi F., Boudhar, A., Benhadj, I, Hanich, L., Benkaddour, A., Guemouria, N., Chehbouni, Ah., Lahrouni, A, Olioso, A., Jacob ,F., Williams, D.G., Sobrino, J.: An integrated modelling and remote sensing approach for hydrological study in arid and semi-arid regions: the SUDMED Programme. International Journal of Remote Sensing. 29, 17 & 18 : 5161 – 5181, 2008.

765 Choudhury, B. J. and Monteith, J. L.: A four-layer model for the heat budget of homogeneous land surfaces. Q. J. Roy. Meteor. Soc., 114:373–398, 1988.
Choudhury, B. J., and Idso, S. B: An empirical model for stomatal resistance of field-grown wheat.Agric. For. Meteorol., 36, 65-82, 1985.
Clapp, R. B., and G. M. Hornberger: Empirical equations for some soil hydraulic properties, Water Resour. Res., 14, 601-
770 604, 1978.
Claussen, M.: Estimation of Areally-Averaged Surface Fluxes, Boundary-Layer Meteorol. 54, 387-410, 1991.
Collins, D.C., Avissar, R.: An evaluation with the Fourier amplitude sensitivity test (FAST) of which land-surface parameters are of greatest importance in atmospheric modelling. J. Climate 7, 681–703, 1994.
Cosby BJ, Hornberger GM, Clapp RB, Ginn TR: A statistical exploration of soil moisture characteristics to the physical
775 properties of soils. Water Resources Research 20, 682–690, 1984.
Coudert, B., Ottlé, C., Boudevillain, B., Demarty, J., and Guillevic, P.: Contribution of Thermal Infrared Remote Sensing Data in Multiobjective Calibration of a Dual-Source SVAT Model, Journal of Hydrometeorology, 7, 404–420, 2006.
Deardorff, J. W.: A parameterization of ground-surface moisture content for use in atmosphere prediction models, J.
780 Appl. Meteor., 16, 1182–1185, 1977.
Deardroff J.W.: Efficient prediction of ground surface temperature and moisture, with inclusion of a layer of vegetation. J. Geophys. Res., 83:1889-1903, 1978.
Decharme, B., Boone, A., Delire, C., and Noilhan, J.: Local evaluation of the interaction between soil biosphere atmosphere soil multilayer diffusion scheme using four pedotransfer functions. J. Geophys.Res., 116(D20),
785 DOI: 10.1029/2011JD016002, 2011.
Decharme, B., Martin, E., and Faroux, S.: Reconciling soil thermal and hydrological lower boundary conditions in land surface models, *J. Geophys. Res.-Atmos*., 118, 7819–7834, https://doi.org/10.1002/jgrd.50631, 2013.
Delire, C., Calvet, J.-C., Noilhan, J., Wright, I., Manzi, A., and Nobre, C.: Physical properties of Amazonian soils: A modeling study using the Anglo-Brazilian Amazonian Climate Observation Study data, J. Geophys. Res., 102,
790 30119–30133, doi:10.1029/97JD01836, 1997.
Demarty, J.: Développement et application du modèle SiSPAT-RS à l'échelle de la parcelle et dans le cadre de l'expérience alpilles ReSeDA. Thèse de doctorat de l'université Denis Diderot de Paris 7, Paris, France, 221 p, 2001.
Demarty, J., C. Ottlé, I. Braud, A. Olioso, J. P. Frangi, H. V. Gupta, and L. A. Bastidas.: Constraining a physically based Soil-Vegetation-Atmosphere Transfer model with surface water content and thermal infrared brightness
795 temperature measurements using a multiobjective approach. WATER RESOURCES RESEARCH, VOL. 41, W01011, doi:10.1029/2004WR003695, 2005.
Dickinson, R.E.: Modeling evapotranspiration for three-dimensional global climate models. American Geophysical Union, Washington D.C.. 29: 5-2. doi: 10.1029/GM029p0058, 1984.
Dolman, A. J.: A Multiple-Source Land Surface Energy Balance Model for Use in General Circulation Models.
800 Agricultural and Forest Meteorology, 65 (1–2), 21–45, 1993.
Duchemin, B., Hadria, R., Er-Raki, S., Boulet, G., Maisongrande, P., Chehbouni, A., Escadafal, R., Ezzahar, J., Hoedjes, J.C.B., Karrou, H., Khabba, S., Mougenot, B., Olioso, A., Rodriguez, J-C., Simonneaux, V.: Monitoring wheat phenology and irrigation in Central Morocco: on the use of relationship between evapotranspiration, crops coefficients, leaf area index and remotely-sensed vegetation indices. Agricultural Water Management, 79, 1- 27,
805 2006.
Duchemin, B., Hagolle O., Mougenot B., Simonneaux V., Benhadj I., Hadria R., Ezzahar J., Hoedjes J., Khabba S., Kharrou M.H, Boulet G., Dedieu G., Er-Raki S., Escadafal R., Olioso A., Chehbouni A.G., 2008. Agrometerological study of semi-arid areas: an experiment for analysing the potential of FORMOSAT-2 time series of images in the Tensift-Marrakech plain. International Journal of Remote Sensing. Vol, 29, pp. 5291 –
810 5299, 2008.

Dunin, F.X., Meyer, W.S., Wong, S.C. and Reyenga, W.: Seasonal change in water use and carbon assimilation of irrigated wheat. Agric. For. Meteorol., 45, 231-250, 1989.

Elammari, A.: Optimisation multi-objectifs et multicritères des paramètres de deux modèles SVAT appliquée à des données semi-arides. Rapport de fin d'études, Ecole Nationale de la Météorologie. 67p, 2008.

Eltahir, E.A.B. : Precipitation Recycling. Rev. Geophys. doi:10.1029/96rg01927, 1996.

Er-Raki, S. , Chehbouni, A., Boulet, G., Williams,D.G. : Using the dual approach of FAO-56 for partitioning ET into soil and plant components for olive orchards in a semi-arid region. Agricultural Water Management. 97, 1769-1778, 2010.

Er-Raki, S.: Estimation des besoinsen eau des cultures dans la région de Tensift AL Haouz : Modélisation, Expérimentation et Télédétection. Thèse de doctorat, Université Cadi Ayyad, Marrakech, Maroc, 128p, 2007.

Er-Raki, S., Chehbouni, A., Guemouria, N., Duchemin, B., Ezzahar, J., and Hadria, R.: Combining FAO-56 model and ground-based remote sensing to estimate water consumptions of wheat crops in a semi-arid region. Agricultural Water Management, 87, 41-54, 2007.

Ezzahar, J., Chehbouni, A., Hoedjes, J.C.B., Er-Raki, S., Chehbouni, Ah., and J-M, Bonnefond, and De Bruin, H.A.R. The use of the Scintillation Technique for estimating and monitoring water consumption of olive orchards in a semi-arid region. Agricultural Water Management, 89, 173-184, 2007a.

Ezzahar, J., Chehbouni, A., Hoedjes, J.C.B., Chehbouni, Ah : On the application of scintillometry over heterogeneous surfaces. Journal of Hydrology, vol. 334, pp. 493-501, 2007b.

Ezzahar, J., Chehbouni, A., Er-Raki, S., and Hanich,L.: Combining a Large Aperture Scintillometer and estimates of available energy to derive evapotranspiration over several agricultural fields in semi-arid regions. Plant Biosystems. 143, 209-221, 2009a.

Ezzahar J. and Chehbouni A: The use of the scintillometry for validating the spatial and temporal aggregation schema over heterogeneous grid. Agricultural and Forest Meteorology, vol. 149, pp. 2098-2109, 2009b.

Faroux, S., Kaptue Tchuente, A.T.; Roujean, J.-L.; Masson, V.; Martin, E.; Le Moigne, P.: ECOCLIMAP-II/Europe: A twofold database of ecosystems and surface parameters at 1 km resolution based on satellite information for use in land surface, meteorological and climate models. Geosci. Model Dev. 6, 563–582, 2013.

Fernández JE, Palomo MJ, Díaz-Espejo A, Clothier BE, Green SR, Girón IF, Moreno F.: Heat-pulse measurements of sap flow in olives for automating irrigation: tests, root flow and diagnostics of water stress. Agric Water Manag 51:99–123, 2001.

Fernandez, J.E., Moreno, F. and Martin-Aranda, J.: Study of root dynamics of olive trees under drip irrigation and dry farming. Acta Hortic. 286, 263–266, 1990.

Garratt, J.R.: The Atmospheric Boundary Layer. Cambridge Univ. Press, Cambridge, U.K., 316 pp, 1992.

Garrigues S., A. Boone, B. Decharme, A. Olioso, C. Albergel, J.-C. Calvet, S. Moulin, S. Buis, and E. Martin: Impacts of the Soil Water Transfer Parameterization on the Simulation of Evapotranspiration over a 14-Year Mediterranean Crop Succession, *Journal of Hydro-Meteorology*, 19, 3-25, 2018.

Garrigues, S., Olioso, A., Carre, D., Decharme,B., Calvet, J.-C. , Martin, E., Moulin, S., and Marloie, O.: Impact of climate, vegetation, soil and crop management variables on multi-year ISBA-A-gs simulations of evapotranspiration over a Mediterranean crop site. Geosci. Model Dev., 8, 3033–3053, 2015.

Gentine, P., Entekhabi, D. Chehbouni, A., Boulet, G. and Duchemin, B.: Analysis of evaporative fraction diurnal behaviour. Agricultural and Forest Meteorology, 143(1-2), 13–29, 2007.

Giordani, H., Noilhan, J., Lacarrere, P. and Bessemoulin, P.: Modeling the surface processes and the atmospheric boundary layer for semi-arid conditions. Agric. For. Meteor., 80, 263–287, 1996.

Goldberg, D.E.: Genetic algorithms in Search, Optimization and Machine learning, 412 pp., Addison-Wesley Publishing Co, Reading, MA, 1989.

Habets, F., Boone, A., Champeaux, J.-L., Etchevers, P., Franchisteguy, L., Leblois, E., Ledoux, E., Le Moigne, P., Martin, E., ´ Morel, S., Noilhan, J., Quintana Segu´ı, P., Rousset-Regimbeau, F., and Viennot, P.: The SAFRAN-ISBA-MODCOU hydrometeorological model applied over France, J. Geophys. Res., 113, D06113, doi:10.1029/2007JDOO8548, 2008.

Hartmann, D.L., Global Physical Climatology, pp 498, 2016, doi:10.1016/B978-0-12-328531-7.00011-6.

Hoedjes, J.C.B., Chehbouni, A., Ezzahar, J., Escadafal, R. and De Bruin, H.A.R: Comparison of Large Aperture Scintillometer and Eddy Covariance Measurements: Can Thermal Infrared Data be Used to Capture Footprint Induced Differences. Journal of Hydrometeorology 8, 144–159, 2007.

Hoedjes, J.C.B, Chehbouni, A., Jacob, F., Ezzahar, J., Boulet G.: Deriving daily evapotranspiration from remotely sensed instantaneous evaporative fraction over olive orchard in semi-arid Morocco. Journal of Hydrology, vol. 354, pp. 53-64, 2008.

Horst, T.W.: On frequency response corrections for eddy covariance flux measurements. Boundary-Layer Meteorol. 95, 517–520, 2000.

Huntingford, C.; Allen, S. J.; Harding, R. J.: An intercomparison of single and dual-source vegetation-atmosphere transfer models applied to transpiration from sahelian savannah. Boundary-Layer Meteorology, 74 (4), 397-418, 1995.

Jackson, R. B., J. Canadell, J. R. Ehleringer, H. A. Mooney, O. E. Sala, and E. D. Schulze: A global analysis of root distributions for terrestrial biomes. Oecologia, 108, 389–411, https://doi.org/10.1007/BF00333714, 1996.

Jacobs, C. M. J.: Direct impact of atmospheric CO_2 enrichment on regional transpiration. PhD. Thesis, Agriculture University , Wageningen, 192 p, 1994.

Jarlan L., Khabba S., Er-Raki S., Le Page M.: Remote Sensing of Water Resources in Semi-Arid Mediterranean Areas: the joint international laboratory TREMA, International Journal of Remote Sensing, 36:19-20, 4879-4917, DOI: 10.1080/01431161.2015.1093198, 2015.

Jasechko Scott, Zachary D. Sharp , John J. Gibson, S. Jean Birks, Yi Yi & Peter J. Fawcett: Terrestrial water fluxes dominated by transpiration. Nature 496, 347–350, 2013.

Jasechko, S., Sharp, Z.D., Gibson, J.J., Birks, S.J., Yi, Y., Fawcett, P.J.: Terrestrial water fluxes dominated by transpiration. Nature 2–6. doi:10.1038/nature11983, 2013.

Jiménez, C., Prigent, C., Mueller, B., Seneviratne, S. I., McCabe, M. F., Wood, E. F., Rossow, W. B., Balsamo, G., Betts, A. K., Dirmeyer, P. A., Fisher, J. B., Jung, M., Kanamitsu, M., Reichle, R. H., Reichstein, M., Rodell, M., Sheffield, J., Tu, K., and Wang, K.: Global intercomparison of 12 land surface heat flux estimates. J. Geophys. Res., 116, D02102, doi:10.1029/2010JD014545, 2011.

Kalma JD, Jupp DLB.: Estimating evaporation from pasture using infrared thermometry: evaluation of a one-layer resistance model. Agric For Meteorol 51:223–246. doi:10.1016/0168-1923(90)90110-R, 1990.

Kim, J., Verma S.B. and Rosenberg, N.J.: Energy balance and water use of cereal crops. Agric. For. Meteorol., 48, 135-147, 1989.

Kool, D., Agam, N., Lazarovitch, N., Heitman, J.L., Sauer, T.J., Ben-Gal, A.: A review of approaches for evapotranspiration partitioning. Agric. For. Meteorol. 184, 56–70, http://dx.doi.org/10.1016/j.agrformet.2013.09.003, 2014.

Lafore, J. P., J. Stein, N. Asencio, P. Bougeault, V. Ducrocq, J. Duron, C. Fischer, P. Hereil, P. Mascart, J. P. Pinty, J. L. Redelsperger, E. Richard, and J. Vila-Guerau de Arellano: The Meso-NH Atmospheric Simulation System. Part I: Adiabatic formulation and control simulations. Annales Geophysicae, 16, 90-109, 1998.

Lawston, P. M., J. A. Santanello, B. Zaitchik, and M. Rodell: Impact of irrigation methods on land surface model spinup and initialization of WRF forecasts. J. Hydrometeor., 16, 1135–1154, doi:10.1175/JHM-D-14-0203.1, 2015.

Le Page, M.; Toumi, J.; Khabba, S.; Hagolle, O.; Tavernier, A.; Kharrou, M.H.; Er-Raki, S.; Huc, M.; Kasbani, M.; Moutamanni, A.E.; Yousfi, M.; Jarlan, L. A Life-Size and Near Real-Time Test of Irrigation Scheduling with a Sentinel-2 Like Time Series (SPOT4-Take5) in Morocco. Remote Sens. 6, 11182-11203, 2014.

Lei H., Yang D. Interannual and seasonal variability in evapotranspiration and energy partitioning over an irrigated cropland in the North China Plain. Agricultural and Forest Meteorology 150, 581–589.

Lhomme J.-P., Monteny B., Amadou M.: Estimating sensible heat flux from radiometric temperature over sparse millet. Agricultural and Forest Meteorology 68 : 77-91, 1994.

Lhomme Jean-Paul, Chehbouni Abdelghani.: Comments on dual-source vegetation-atmosphere transfer models. Agricultural and Forest Meteorology, 94 (3-4), p. 269-273. ISSN 0168-1923, 1999.

Lhomme, J. P., Montes, C., Jacob, F., and Prévot, L.: Evaporation from heterogeneous and sparse canopies: on the formulations related to multi-source representations, Bound.-Lay. Meteorol., 144, 243–262, 2012.

Lhomme, J.P., Troufleau, D., Monteny, B., Chehbouni, A., Bauduin, S.: Sensible heat flux–radiometric surfacetemperature over sparse Sahelian vegetation. II. A model for the kB−1 parameter. J. Hydrol. 188–189, 839–854, 1997.

Liu, C.M., Zhang, X.Y., Zhang, Y.Q.: Determination of daily evaporation andevapotranspiration of winter wheat and maize by large-scale weighinglysimeter and micro-lysimeter. Agric. Forest Meteorol. 111, 109–120, 2002.

Louis, J.-F.: A parametric model of vertical eddy fluxes in the atmosphere. Boundary-LayerMeteorology, 17(2), 187–202, 1979.

Maillard P., L'olivier. Comité technique de l'olivier section spécialise de l'INVFLEC. Paris, 137 p. 1975

Manzi, A.O. and Planton, S.: Implementation of the isba parameterization scheme for land surface processes in a gcm-an annual cycle experiment. J. Hydrol., 155, 353–387, 1994.

Masson, V., Le Moigne, P., Martin, E., Faroux, S., Alias, A., Alkama, R., Belamari, S., Barbu, A., Boone, A., Bouyssel, F.: The surfex v7. 2 land and ocean surface platform for coupled or offline simulation of earth surface variables and fluxes. Geoscientific Model Development, 6, 929–960, 2013.

Napoly, A., Boone, A., Samuelsson, P., Gollvik, S., Martin, E., Seferian, R., Carrer, D., Decharme, B., & Jarlan, L.: The interactions between soil–biosphere–atmosphere (ISBA) land surface model multi-energy balance (MEB) option in SURFEXv8 – Part 2: Introduction of a litter formulation and model evaluation for local-scale forest sites. *Geosci. Model Dev.*, *10*, 1621-1644, 2017.

Noilhan J., Mahfouf J.-F.: The ISBA land surface parameterisation scheme. Global and Planetary Change, vol 13, pp.145-159, 1996.

Noilhan, J. and Planton, S.: A simple parameterization of land surface processes for meteorological models. Mon. Wea. Rev., 117:536–549, 1989.

Norman, J.M., Kustas, W.P., Humes, K.S.: Two source approach for estimating soil and vegetation energy fluxes in observations of directional radiometric surface temperature. Agric. For. Meteorol. 77, 263–293, 1995.

Ogée J, Brunet Y, Loustau D, Berbigier P, Delzon S: Water and energy multilayer, multileaf pine forest model: evaluation from hourly to yearly time scales and sensitivity analysis. Global Change Biology, 9, 697–717, 2003.

Oishi, A.C., Oren, R., Stoy, P.C.: Estimating components of forest evapotranspiration: a footprint approach for scaling sapflux measurements. Agricultural and Forest Meteorology, 148, 1719–1732, 2008.

Olioso, A., H. Autret, O. Bethenot, J.M. Bonnefond, I. Braud, J.C. Calvet, A. Chanzy, D. Courault, J. Demarty, Y. Ducros, J.C. Gaudu, E. Gonzales-Sosa, R. Gouget, R. Jongschaap, Y. Kerr, J.P. Lagouarde, J.P. Laurent, E. Lewan, O. Marloie, J. Mc Anneney, S. Moulin, C. Ottlé, L. Prévot, J.L. Thony, J.P. Wigneron, and W. Zhao. Comparison of SVAT models over the Alpilles-ReSeDA experiment. II Models and Results. Physics and Chemistry of the Earth(B), 2001.

Oren, R, Sperry, JS., Katul, GG., Pataki, DE., Ewers, BE., Phillips, N., Schäfer, KVR.: Intra- and interspecific responses of canopy stomatal conductance to vapour pressure deficit. Plant Cell Environ 22, 1515–1526, 1999.

Ozdogan, M., M. Rodell, H. K. Beaudoing, and D. L. Toll: Simulating the effects of irrigation over the United States in a land surface model based on satellite-derived agricultural data, J. Hydrometeorol., 11(1), 171–184, doi:10.1175/2009JHM1116.1, 2010.

Pianosi F., T. Wagener, J. Rougier, J. Freer, J. Hall: Sensitivity analysis of environmental models: a systematic review with practical workflow .Vulnerability, Uncertainty, and Risk, pp. 290-299, 2014.

Poblete-Echeverría, C., Ortega-Farias, S.: Estimation of actual evapotranspiration for a drip-irrigated Merlot vineyard using a three-source model. Irrig. Sci. 28, 65–78, 2009.

Raupach MR, Finnigan JJ.: Single-layer models of evaporation from plant canopies are incorrect but useful, whereas multilayer models are correct but useless: discuss. Aust J Plant Physiol 15:705– 716, 1988.

Raupach, M.R.: Vegetation-atmosphere interaction in homogeneous and heterogeneous terrain: some implications of mixed-layer dynamics. Vegetation, 91, 105-120, 1991.

Rivalland, V., Calvet, J.-C., Berbigier, P., Brunet, Y., and Granier, A.: Transpiration and CO_2 fluxes of a pine forest: modelling the undergrowth effect. Ann. Geophys., 23, 291–304, 2005.

Roupsard O., Bonnefond J., Irvine M., Berbigier P., Nouvellon Y., Dauzat J., Taga S., Hamel O., Jourdan C., Saint-André L., Mialet-Serra I., Labouisse J.P., Epron D., Joffre R., Braconnier S., Rouzière A., Navarro M., Bouillet J.P.: Partioning energy and evapo-transpiration above and below a tropical palm canopy, Agricultural and Forest Meteorology, 139, 252-268, 2006.

Rowntree, PR : Atmospheric parametrization schemes for evaporation over land: basic concepts and climate modeling aspects. In: land surface evaporation: measurements and parametrization (Schmugge TJ, Andre JC ed), Springer-Verlag New York 5-29, 1991.

Ryder, J., Polcher, J., Peylin, P., Ottlé, C., Chen, Y., van Gorsel, E., Haverd, V., McGrath, M. J., Naudts, K., Otto, J., Valade, A., and Luyssaert, S.: Amulti-layer land surface energy budget model for implicit coupling with global atmospheric simulations. Geosci.Model Dev., 9:223–245, 2016.

Séférian, R., Delire, C., Decharme, B., Voldoire, A., Salas y Mélia, D., Chevallier, M., Saint-Martin, D., Aumont, O., Calvet, J.-C., Carrer, D., Douville, H., Franchistéguy, L., Joetzjer, E. and Sénési, S.: Development and evaluation of CNRM Earth-System model – CNRM-ESM1, Geosci. Model Dev. Discuss., 8(7), 5671–5739, 2015.

Seity, Y., Brousseau, P., Malardel, S., Hello, G., Benard, P., Bouttier, F., Lac, C., ´ and Masson, V.: The AROME-France convective-scale operational model. Mon. Wea. Rev., 139:976–991, 2011.

Sellers, P. J., Mintz, Y., Sud, Y. C., and Dalcher, A.: A simple biosphere model (SiB) for use within general ciculation models. J. Atmos. Sci., 43, 505–531, 1986.

Sellers, P.J., Los, S.O., Tucker, C.J.: A revised land-surface parameterization (SiB2) for atmospheric GCMs. Part 2: The generation of global fields of terrestrial biophysical parameters from satellite data, Journal of Climate, 9, 706–737, 1996.

Shawcroft, R.W., and Gardner, H.R.: Direct evaporation from soil under a row crop canopy, Agric. Meteorol., 28, pp. 229-238, 1983.

Shuttleworth,W. J., &Wallace, J. S.: Evaporation from sparse crops-an energy combination theory. Quarterly Journal of the Royal Meteorological Society, 111(469), 839–855, 1985.

Shuttleworth, W.J. and Gurney, R.J.: The theoretical relationship between foliage temperature and canopy resistance in sparse crops. Q.J.R. Meteorol. Soc., 116: 497-519, 1990.

Stannard, D.I., and Weltz, M.A: Partitioning evapotranspiration in sparsely vegetated rangeland using a portable chamber: Water Resources Research, v. 42, doi:10.1029/2005WR004251, 2006.

Twine, T.E., Kustas, W.P., Norman, J.M., Cook, D.R., Houser, P.R., Meyers, T.P., Prueger, J.H., Starks, P.J., and Wesly, M.L.: Correcting Eddy-Covariance Flux Underestimates over a Grassland. Agric. For. Meteorol. 103, 279-300, 2000.

Taylor K. E.: Summarizing multiple aspects of model performance in a single diagram.Journal of Geophysical Research, 106, 7183-7192, 2001.

Van den Hurk, B.J.J.M, and McNaughton, K.G.: Implementation of near-field dispersion in a simple two-layer surface resistance model. Journal of Hydrology 166: 293: 311, 1995.

Verseghy, D., McFarlane, N., and Lazare, M.: Class a canadian land surface scheme for gcms, ii. vegetation model and coupled runs. International Journal of Climatology, 13(4), 347–370, 1993.

Vogel, Christoph A., Dennis D. Baldocchi, Ashok K. Luhar, and K. Shankar Rao.: A Comparison of a Hierarchy of Models for Determining Energy Balance Components over Vegetation Canopies.Journal of Applied Meteorology.34, 2182-2196, 1995.

Voldoire, A., Sanchez-Gomez, E., Salas y Mélia, D., Decharme, B., Cassou, C., Sénési, S., Valcke, S., Beau, I., Alias, A., Chevallier, M., Déqué, M., Deshayes, J., Douville, H., Fernandez, E., Madec, G., Maisonnave, E., Moine, M.-P., Planton, S., SaintMartin, D., Szopa, S., Tyteca, S., Alkama, R., Belamari, S., Braun, A., Coquart, L., and Chauvin, F.: The CNRM-CM5.1 global climate model: description and basic evaluation, Clim. Dynam., 40, 2091-2121, doi:10.1007/s00382-011-1259-y, 2013.

Voltz M, Ludwig W., Leduc C., Bouarfa S.: Mediterranean land systems under global change: current state and future challenges. Regional Environmental Change. 18:619-622, 2018.

Wang, P., Song, X., Han, D., Zhang, Y., Zhang, B.: Determination of evaporation, transpiration and deep percolation of summer corn and winter wheat after irrigation. Agric. Water Manage. 105, 32–37, 2012.

Wang, W.G., Xing, W.Q., Shao, Q.X., Yu, Z.B., Peng, S.Z., Yang, T., Yong, B., Taylor, J., Singh, V.P.: Changes in reference evapotranspiration across the Tibetan Plateau: Observations and future projections based on statistical downscaling. J. Geophys. Res. Atmos. 118(10), 4049-4068. http://dx.doi.org/10.1002/jgrd.50393, 2013.

Wang, X.F. and D. Yakir.: Using stable isotopes of water in evapotranspiration studies. Hydrol. Process. 14: 1407-1421, 2000.

Williams, D.G., Cable, W., Hultine, K., Hoedjes, J.C.B., Yepez, E.A., Simonneaux, V., Er-Raki, S., Boulet, G., de Bruin, H.A.R., Chehbouni, A., Hartogensis, O.K., Timouk, F.: Components of evapotranspiration in an olive orchard determined by eddy covariance, sap flow and stable isotope techniques. Agricultural and Forest Meteorology. 125, 241–258, 2004.

Xu C.Y., E. Widén, S. Halldin: Modelling hydrological consequences of climate change-progress and challenges Adv. Atmos. Sci., 22 (6), pp. 789-797, 10.1007/BF02918679, 2005.

Xu C.Y., V.P. Singh: Evaluation of three complementary relationship evapotranspiration models by water balance approach to estimate actual regional evapotranspiration in different climatic regions. J. Hydrol., 308, pp. 105-121, 10.1016/j.jhydrol.2004.10.024, 2005.

Yakir, D., Sternberg L. da L.S.: The use of stable isotopes to study ecosystem gas exchange. Oecologia. 123, 297–311, 2000.

Yucui, Z.,Yanjun, S., Hongyong, S., John, B.G.: Evapotranspiration and its partitioning in an irrigated winter wheat field: A combined isotopic and micrometeorologic approach. Journal of Hydrology. 408, 203-211, 2011.

1025

Tables

Table 1: Overview of the different micrometeorological instruments used over the two sites.

Sites	Agdal	R3
Seasons	2003 and 2004	2002-2003 and 2012-2013
Air temperature and relative humidity	Vaisala HMP45AC (9 m)	Vaisala HMP45AC (2 m)
Wind speed and direction	Young Wp200 (9 m)	Young Wp200 (3 m)
Net radiation (Sol +Vegetation)	CNR1 radiometer (Kipp & Zonen) (8.5 m)	CNR1 radiometer (Kipp & Zonen) (2 m)
Soil net radiation	Q6 radiometer (REBS) (1m)	
Vegetation net radiation	Q7 radiometer (REBS) (7 m)	
Radiative soil and vegetation temperatures	Precision Infrared temperature sensor (IRTS-P) (1 and 7.15 m)	Precision Infrared temperature sensor (IRTS-P) (2 m)
Soil moisture	CS616 water content reflectometer (5, 10, 20, 30, 40 cm) and gravimetric technique	CS616 water content reflectometer (5, 10, 20, 30, 40 cm) and gravimetric technique
Soil heat flux	Heat flux plates (HFT3-L) (1 cm)	Heat flux plates (HFT3-L) (5 cm)
Sensible heat flux	3D sonic anemometer (Eddy-covariance method 9.2 m)	3D sonic anemometer (Eddy-covariance method 2 m)
Latent heat flux	Krypton hygrometer (KH20) (Eddy-covariance method 9.2 m)	Open-path infra-red gas analyser (LICOR-7500) (Eddy-covariance method 2 m)
Plant transpiration and soil evaporation	Sapflow (Heat Ratio Method (HRM))	Isotopic method

1030 **Table 2**: Input parameter and variables of the ISBA model derived from *in situ* measurements.

	Olive orchard site	**Wheat site**
Patch	Temperate Broad Leaf Evergreen	Crop C3
Cover fraction (%)	55	Variable
LAI (m^2/m^2)	3	Variable
Vegetation height (m)	6.5	Variable
Emissivity	0.98	0.97
Soil albedo	0.18	0.15
Vegetation albedo	0.14	0.20
Soil texture (%)	44% Sand, 30% Clay	20% Sand, 47% Clay
Root depth (m)	1	0.55

Table 3**: List of parameters used for sensitivity analysis and their considered ranges.**

Name	**Description**	**Parameter range**	**Unit**	**References**
Sd	Sand content	0.39-0.48 (Agdal) 0.18-0.22 (R3)	-	Noilhan and Mahfouf, 1996; Equation (27)
Cl	Clay content	0.27-0.33 (Agdal) 0.42-0.51 (R3)	-	Noilhan and Mahfouf, 1996; Equation (28)
RD	Root depth	0.5-1 (Perennial trees) 0.4-0.7 (C3 crops)	m	ECOCLIMAP
z_o / z_{oH}	Roughness ratio	9-11 (Agdal) 7-11 (R3)	-	Boone et al., 2017; Equation (66)
τ_{LW}	Longwave radiation transmission factor	0.1-0.9	-	Boone et al., 2017; Equation (45)
g_m	Mesophyll conductance	0.0001- 0.04	$m.s^{-1}$	Calvet 2000 ; Equation (A1)
Γ	Coefficient for the calculation of the surface stomatal resistance	0-0.06	$\mu mol\ mol^{-1}$	Calvet 2000 ; Equation (A1)
$W_{r\max}$	Coefficient for maximum water interception storage on capacity on the vegetation	0.05-0.3	mm	Noilhan and planton 1989; Equation (24)

C_v	Thermal coefficient for the vegetation canopy	0.5e-5 - 3e-5	$J.m^2.K^{-1}$	Noilhan and planton 1989; Equation (8)
g_c	Cuticular conductance	0-0.0004	$m.s^{-1}$	Gibelin et al., 2006; Equation (A3)
U_l	Typical value of wind speed	0.5- 3	$m.s^{-1}$	Sellers et al., 1996; Equation (B7)
θ_c	Critical normalized soil water content for stress parameterization	0.1-0.5	–	Calvet 2000 ; Equation (9)
D_{max}	Maximum air saturation deficit	0.03-0.6	$kg.kg^{-1}$	Calvet 2000; Equation (A3)
L_w	Leaf width	0.01-0.04	m	Boone et al., 2017; Equation (51)
ϕ_v	Attenuation coefficient for momentum	1.5-5	–	Boone et al., 2017; Equation (55)
ϕ'_v	Attenuation coefficient for wind	2- 4	–	Boone et al., 2017; Equation (51)

1035

Table 4**: Default values from literature or ECOCLIMAP-II data base and optimal values (see text) of the highly sensitive parameters for one of the objective functions.**

Olive/Agdal	Default values	Optimal values	**Wheat/R3**	Default values	Optimal values
Sand	0.44	0.47	Clay	0.47	0.44
Clay	0.30	0.27	RD	0.50	0.55
RD	1.00	0.62	$\frac{z_0}{z_{0h}}$	10.00	7.01
τ_{LW}	0.50	0.43	τ_{LW}	0.40	0.31
U_l	1.000	2.435	U_l	1.00	1.96
L_w	0.010	0.021	L_w	0.010	0.029
ϕ_v	2.00	4.45	ϕ_v	2.00	3.12

ϕ_v'	3.00	2.12	ϕ_v'	3.00	2.24

Table 5: Comparison between observations and ISBA for the components of the energy balance through Root mean square error (RMSE), correlation coefficient (r) and bias (BIAS). The calibration period is 2003 for both sites while validation is 2004 for Agdal and 2013 for R3.

			Calibration			**Validation**		
			RMSE	r	BIAS	RMSE	r	BIAS
ISBA-1P	**Wheat**	R_n	27.8	0.98	0.9	24.8	0.99	-5.1
		G	19.7	0.83	1.0	32.8	0.68	21.9
		H	55.2	0.71	4.3	31.7	0.62	-10.1
		LE	82.7	0.73	1.9	69.2	0.85	15.8
	Olive orchard	R_n	19.0	0.99	-3.0	14.8	0.99	0.9
		G	22.7	0.73	11.9	42.0	0.75	37.0
		H	76.0	0.68	-9.0	90.3	0.60	-41.9
		LE	86.1	0.52	4.0	107.1	0.67	31.5
ISBA-2P	**Olive orchard**	R_n	17.2	0.99	-3.0	11.0	0.99	-0.7
		G	28.2	0.68	-7.5	17.0	0.78	14.6
		H	40.4	0.85	11.6	47.0	0.83	-12.0
		LE	46.3	0.81	9.4	52.2	0.86	12.7
ISBA-MEB	**Wheat**	R_n	29.0	0.98	-2.8	26.0	0.99	-5.5
		G	32.2	0.65	17.9	55.2	0.79	31.7
		H	55.0	0.66	-10.8	26.2	0.73	0.5
		LE	73.7	0.73	-0.9	56.7	0.92	-8.0
	Olive orchard	R_n	17.7	0.99	-3.0	11.0	1.0	-1.9
		G	29.0	0.69	21.8	54.0	0.74	49.0
		H	39.0	0.85	-0.6	44.0	0.84	-15.0
		LE	38.6	0.83	-4.9	40.2	0.88	-3.4

Table 6 : Percentages of transpiration simulated by the three configurations of the ISBA model and measured by the isotopic method for the 2013 season at the R3 site. The corresponding LAI and F_c are also provided.

	LAI(m^2/m^2)	**F_c**	**T_r (ISBA-1P)**	**T_r(ISBA_MEB)**	**T_r (Observations)**

101	3.8	0.9	73%	85%	83%
102	3.8	0.9	75%	89%	77%

Figures captions

Figure 1: Overview of the two experimental sites: Olive orchard named Agdal and winter wheat named R3.

Figure 2: Schematic description of the three configurations of ISBA model: (a) the single-source configuration (ISBA-1P); (b) the layer configuration (ISBA-MEB); (c) the patch configuration (ISBA-2P).

Figure 3: results of the sensitivity analysis of the ISBA-MEB model for both sites.

Figure 4: Time series of the daily average simulated and measured latent heat flux (LE) for the Agdal site (2003 and 2004 seasons) and for the R3 site (2003 and 2013 seasons).

Figure 5: Taylor diagrams for the net radiation R_n, the sensible heat flux H and the ground heat flux for Agdal (2003 and 2004 seasons) and R3 sites (2003 and 2013 seasons). ISBA-1P is in red, ISBA-2P is in blue, ISBA-MEB is in green and observations are indicated using a black point.

Figure 6: Time series of the daily average soil net radiation (a; only the patch ‘’bare soil’’ is shown for the ISBA-2P configuration), daily average soil temperature (b) and daily average vegetation temperature (c) simulated by the three configurations and measured at the Agdal site for the 2003 season.

Figure 7: Time series of the daily cumulative simulated plant transpiration and measurements by the Sapflow method during the 2004 summer season at the Agdal site.

Figure 8: Comparison between the simulated soil water content with that measured at 5cm at the R3 and Agdal sites during the 2003 season, as well as for the root zone (60cm for the R3 site only).

Figure 9: Time series of simulated and observed surface temperature (T_s), the ground heat flux (G), and the convective heat fluxes (H and LE) during the transient regime around an irrigation event (from 5 days before irrigation and to 8 days after irrigation).

Figures

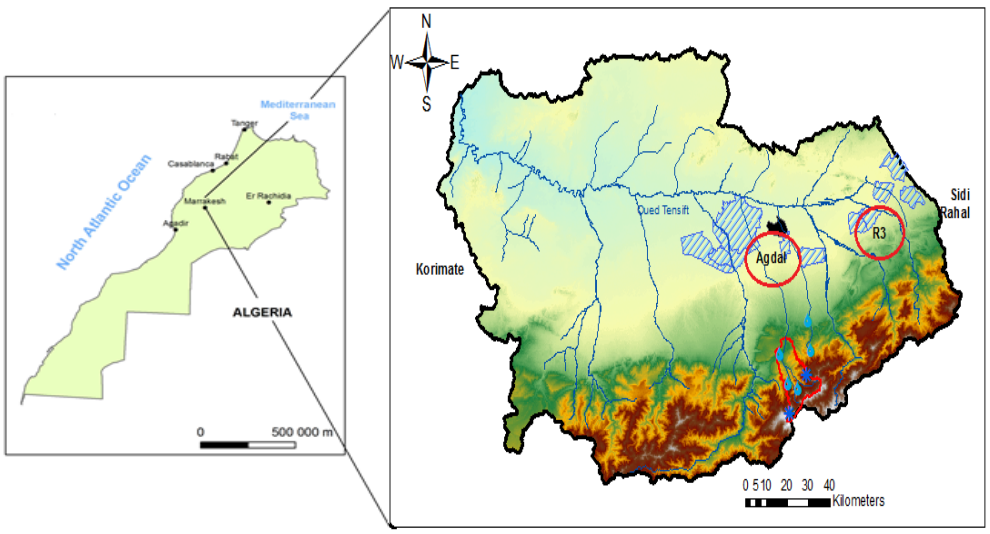

1080

Figure 1

1085

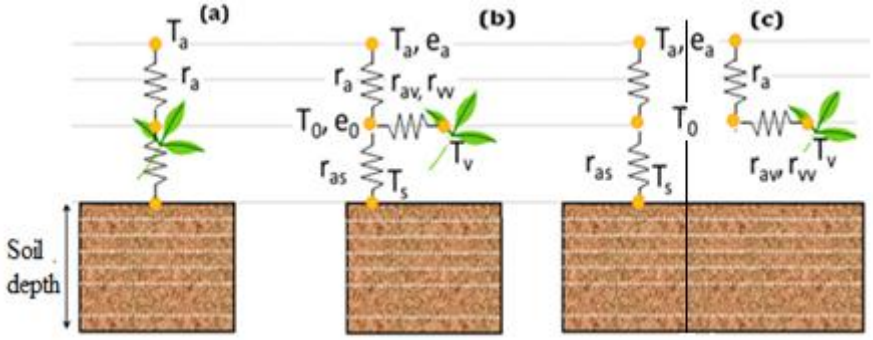

Figure 2

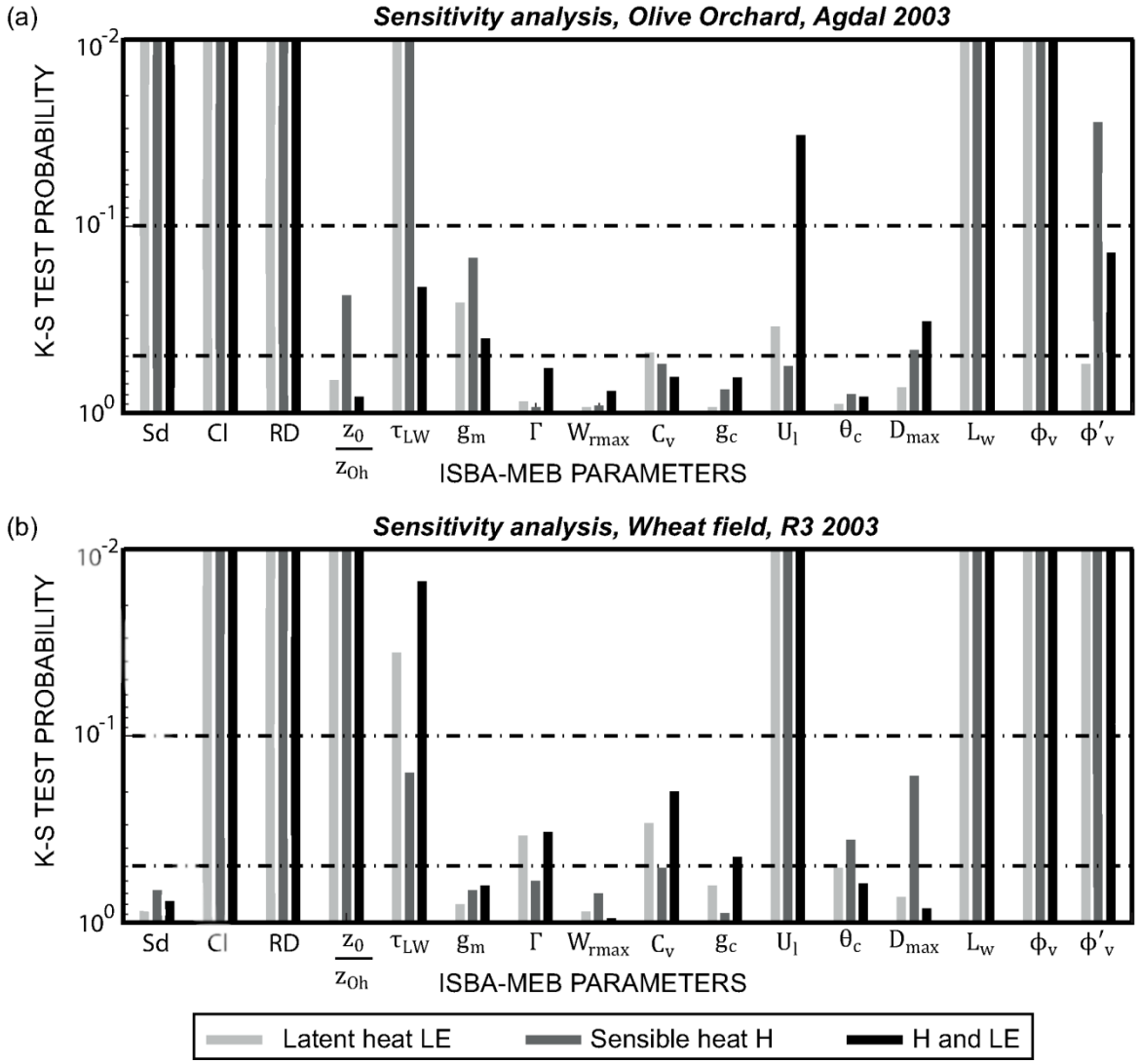

1090 **Figure 3**

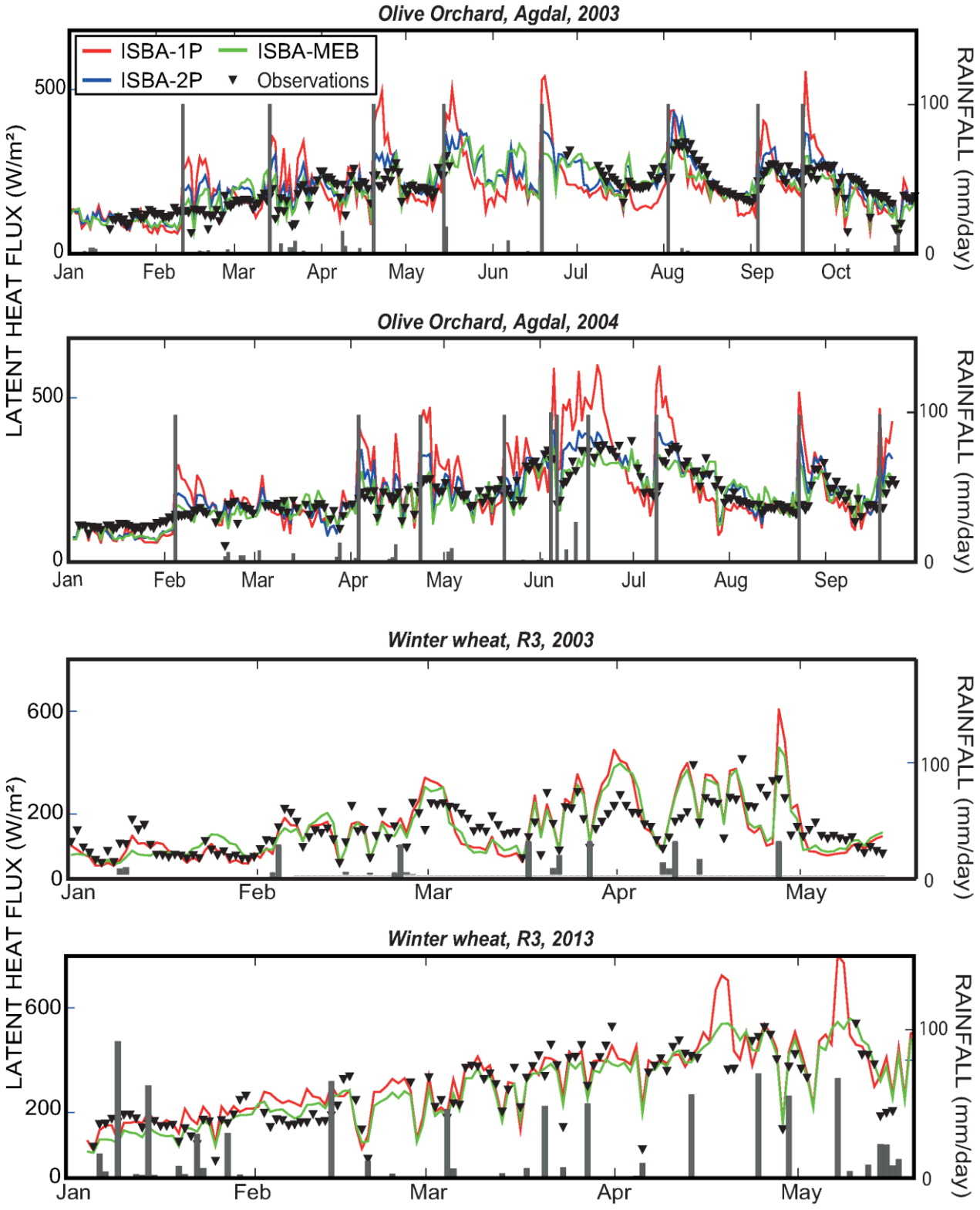
Olive Orchard, Agdal, 2003
ISBA-1P
ISBA-MEB
ISBA-2P
Observations
LATENT HEAT FLUX (W/m²)
RAINFALL (mm/day)
500
0
100
0
Jan
Feb
Mar
Apr
May
Jun
Jul
Aug
Sep
Oct
Olive Orchard, Agdal, 2004
Winter wheat, R3, 2003
600
200
Winter wheat, R3, 2013

Figure 4

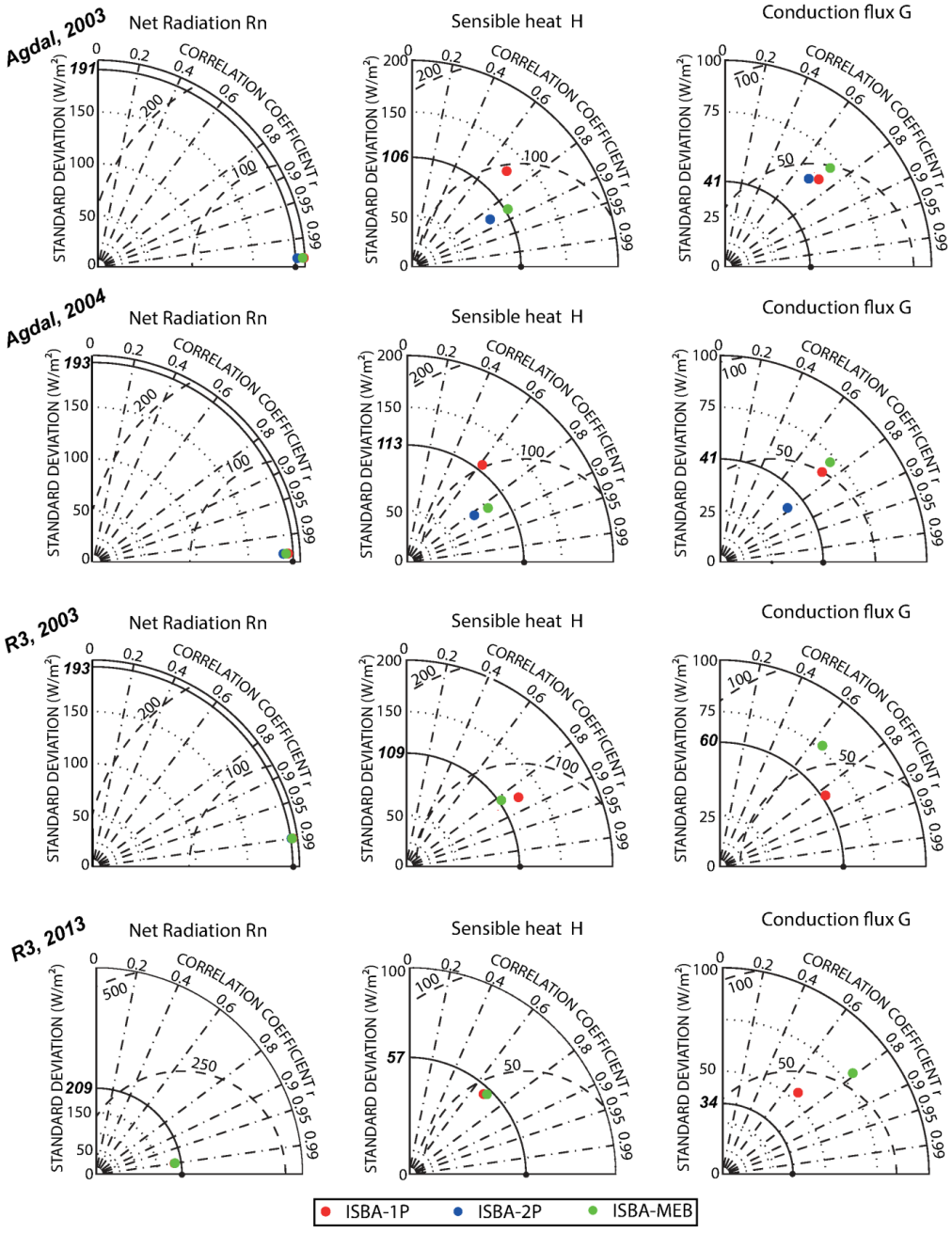

Figure 5

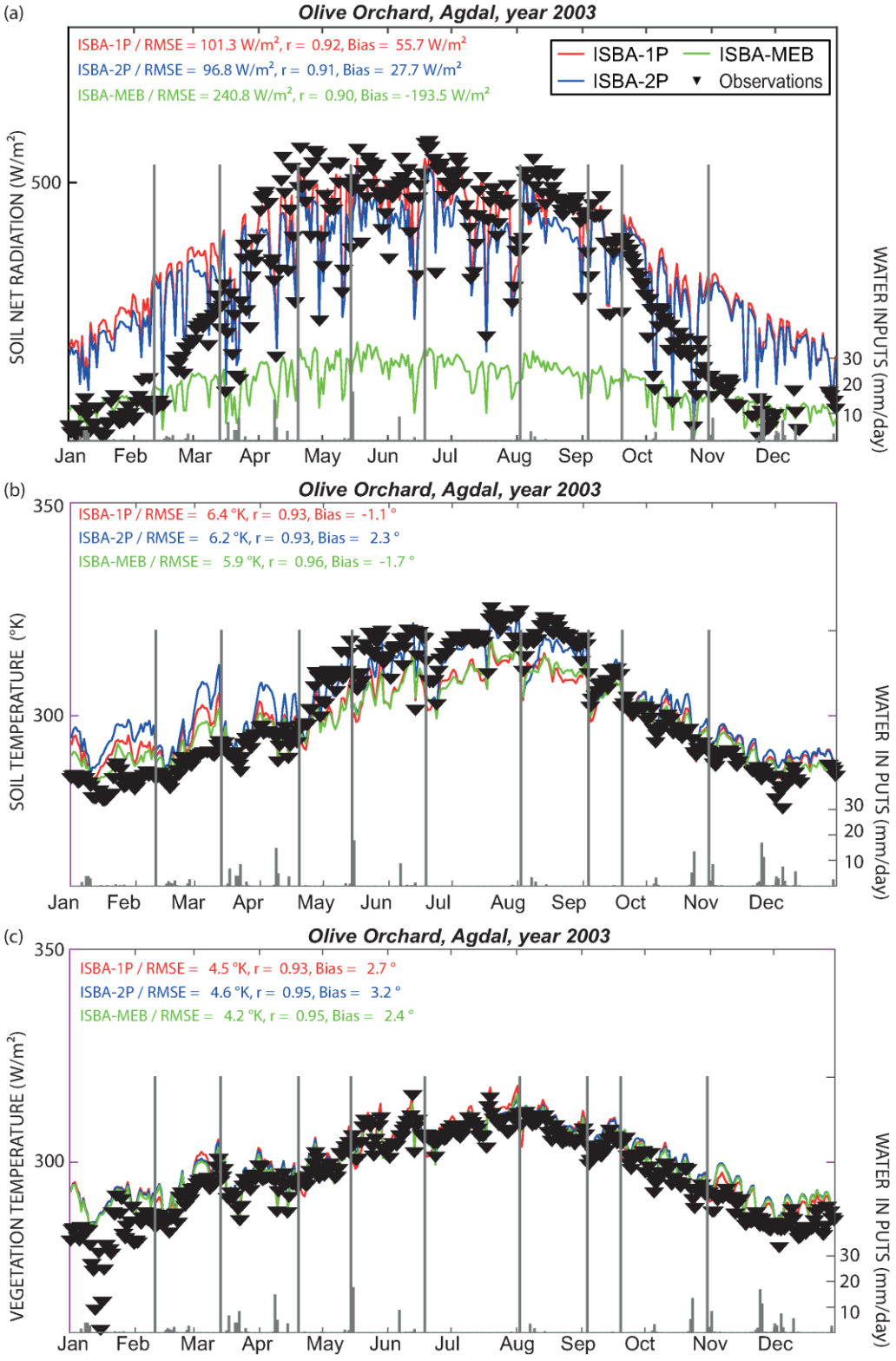
(a)
Olive Orchard, Agdal, year 2003
ISBA-1P / RMSE = 101.3 W/m², r = 0.92, Bias = 55.7 W/m²
ISBA-2P / RMSE = 96.8 W/m², r = 0.91, Bias = 27.7 W/m²
ISBA-MEB / RMSE = 240.8 W/m², r = 0.90, Bias = -193.5 W/m²
ISBA-1P
ISBA-2P
ISBA-MEB
Observations
SOIL NET RADIATION (W/m²)
500
WATER INPUTS (mm/day)
30
20
10
Jan Feb Mar Apr May Jun Jul Aug Sep Oct Nov Dec
(b)
Olive Orchard, Agdal, year 2003
ISBA-1P / RMSE = 6.4 °K, r = 0.93, Bias = -1.1 °
ISBA-2P / RMSE = 6.2 °K, r = 0.93, Bias = 2.3 °
ISBA-MEB / RMSE = 5.9 °K, r = 0.96, Bias = -1.7 °
SOIL TEMPERATURE (°K)
350
300
WATER IN PUTS (mm/day)
30
20
10
Jan Feb Mar Apr May Jun Jul Aug Sep Oct Nov Dec
(c)
Olive Orchard, Agdal, year 2003
ISBA-1P / RMSE = 4.5 °K, r = 0.93, Bias = 2.7 °
ISBA-2P / RMSE = 4.6 °K, r = 0.95, Bias = 3.2 °
ISBA-MEB / RMSE = 4.2 °K, r = 0.95, Bias = 2.4 °
VEGETATION TEMPERATURE (W/m²)
350
300
WATER IN PUTS (mm/day)
30
20
10
Jan Feb Mar Apr May Jun Jul Aug Sep Oct Nov Dec

1095

Figure 6

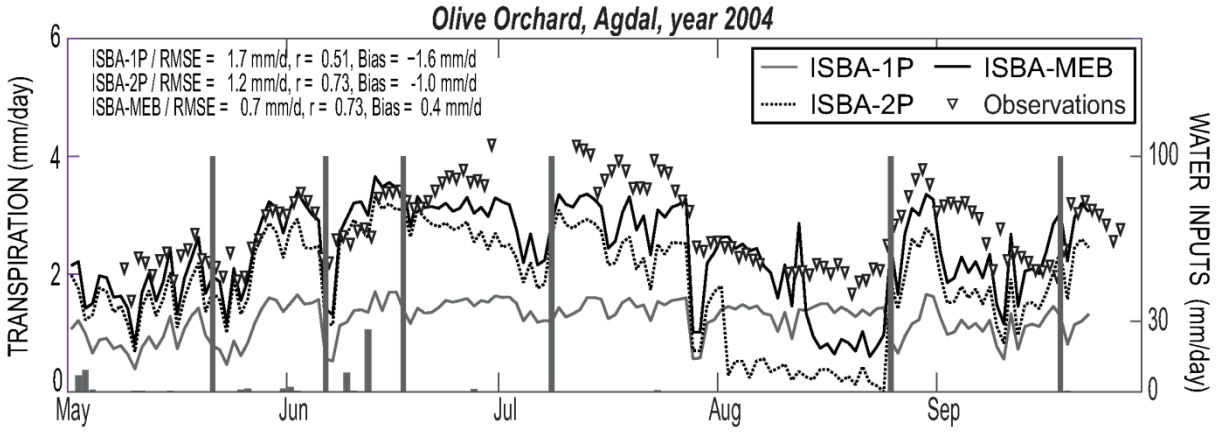

Figure 7

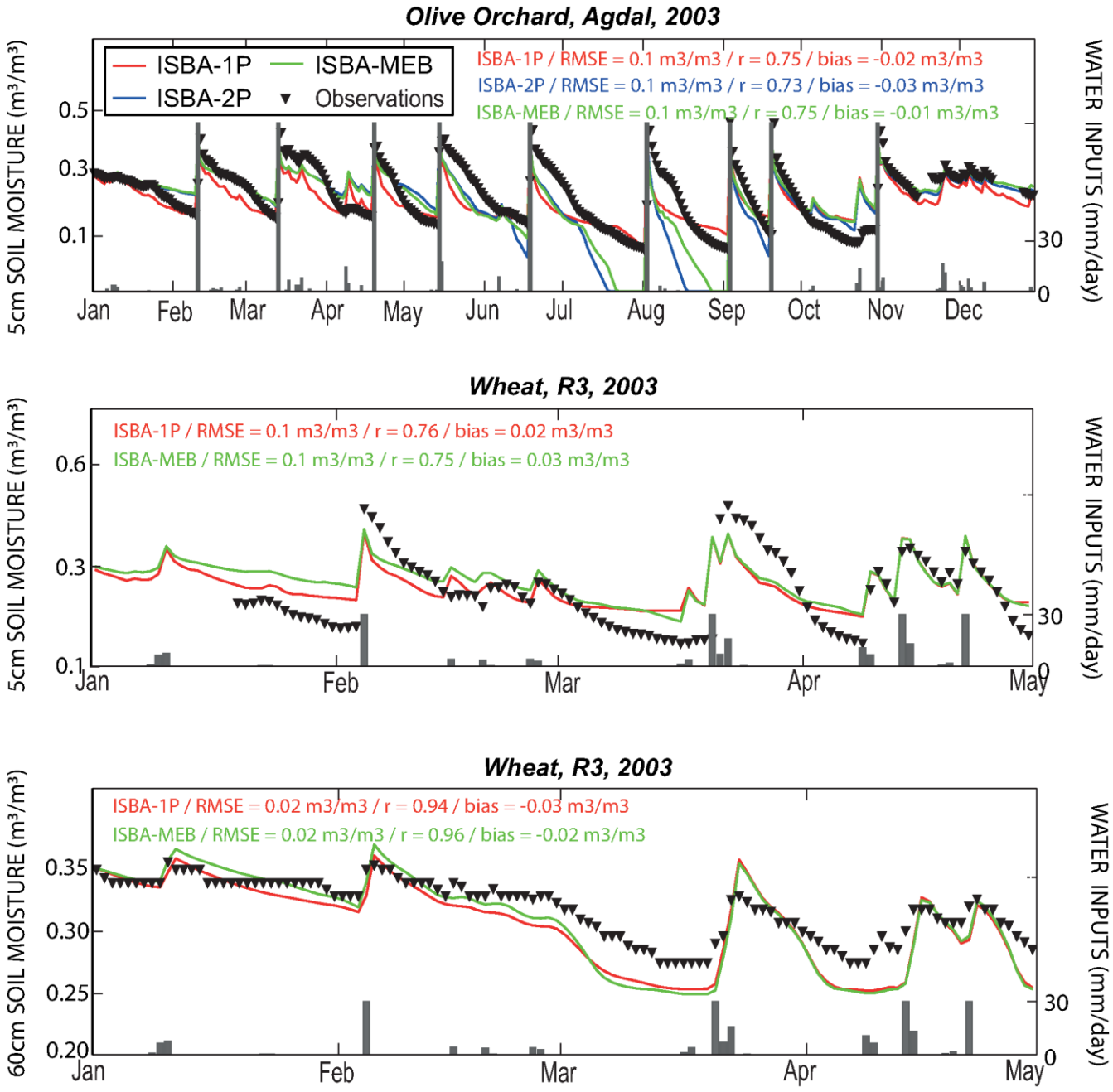

1100 **Figure 8**

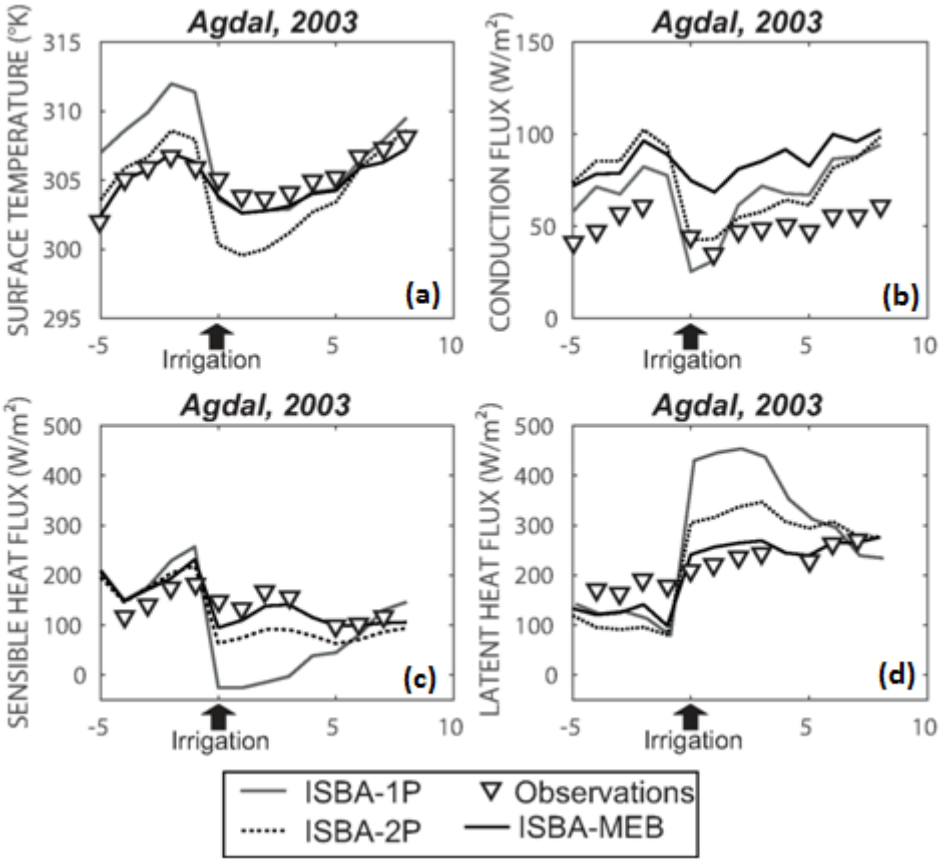

Figure 9

Appendix 1: Prognostic Equations of ISBA-A-gs

Standard version

The governing equations for heat and water transfers within the soil and at the surface are given by the following formulas (More details are provided in Decharme et al., 2011):

$$\frac{\partial T_{g,1}}{\partial t} = C_T G_0 - C_G \frac{\overline{\lambda_1}}{\Delta \tilde{z}_1}\left(T_{g,1} - T_{g,2}\right) \quad (1)$$

$$\frac{\partial T_{g,i}}{\partial t} = \frac{1}{C_{g,i}\Delta_{g,i}}\left[\frac{\overline{\lambda_{i-1}}}{\Delta \tilde{z}_{i-1}}\left(T_{i-1} - T_i\right) - \frac{\overline{\lambda_i}}{\Delta \tilde{z}_i}\left(T_i - T_{i+1}\right)\right] \forall i = 2, N \quad (2)$$

$$\frac{\partial W_{g,1}}{\partial t} = \frac{1}{\rho_w \Delta z_{g,1}} \left[(1 - veg) P_r + D_r - E_g - R - F_{g,1} \right] \quad (3)$$

$$\frac{\partial W_{g,i}}{\partial t} = \frac{1}{\rho_w \Delta z_{g,i}} \left(F_{g,i} - F_{g,i+1} \right) \quad (4)$$

Where $T_{g,1}$ (K) is the uppermost ground temperature and $T_{g,i}$ (K) is the temperature of the layer i; C_T (K.m^{-2}.J^{-1}) is the surface composite thermal inertia coefficient (Noilhan and Planton, 1989); G_0 is the flux between the atmosphere and the surface; $\Delta \tilde{z}_i$ (m) and Δz_i (m) are the thickness between two consecutive layer midpoints or nodes and the thickness of the layer i, respectively; $C_{g,i}$ (J.m^{-3}.K^{-1}) is the heat capacity of the soil, $\overline{\lambda_i}$ (W.m^{-1}.K^{-1}) is the inverse of weighted arithmetic mean of the soil thermal conductivity at the interface between two consecutive nodes and veg is the cover fraction. $F_{g,i}$ represents the vertical flow of water between layers i and i+1 and is given by the Law of Darcy. E_g, D_r, P_r and R are the amount of water evaporated from the soil (Kg.m^{-2}.s^{-1}), rainfall (Kg.m^{-2}.s^{-1}), canopy drainage (Kg.m^{-2}.s^{-1}) and surface runoff (Kg.m^{-2}.s^{-1}).

The soil heat flux, G, is defined as:

$$G = \frac{\overline{\lambda_i}}{\Delta \tilde{z}_i} \left(T_i - T_{i+1} \right) \quad (5)$$

With $\overline{\lambda_i}$ is the thermal conductivity, $\Delta \tilde{z}_i$ the thickness between the center of the first layer and that of the second, T_i the temperature of the first layer and T_{i+1} the temperature of the second layer.

The net radiation is calculated as follows:

$$R_n = R_G (1 - \alpha) + \varepsilon (R_A - \sigma T_s^4) \quad (6)$$

Where α and ε are the albedo and the emissivity, respectively, σ (W.m^{-2}.K^{-4}) is the Stefan Boltzmann constant, R_G is the incoming solar radiation and R_A is the atmospheric radiation.

The sensible heat flux, H, is expressed as follows:

$$H = \rho_a c_p C_H V_a (T_s - T_a) \quad (7)$$

Where ρ_a(Kg.m^{-3}) is the air density, c_p (J.Kg^{-1}.K^{-1}) is the specific heat of the air, V_a (m.s^{-1}) is the wind speed and T_a(k^{-1}) is air temperature, C_H is the drag coefficient.

The latent heat flux LE (W.m-²), the evaporation from the soil (E_g), the direct evaporation from the foliage (E_r) and the transpiration (E_{tr}) are defined as follows:

$$LE = L_v(E_r + E_{tr} + E_g) \quad (8)$$

$$E_g = (1 - veg)\rho_a C_H V_a[h_u q_{sat}(T_s) - q_a] \quad (9)$$

$$E_r = veg\,\frac{\delta}{R_a}\rho_a C_H V_a[q_{sat}(T_s) - q_a] \quad (10)$$

$$E_{tr} = veg\,\frac{1-\delta}{R_a+R_s}\rho_a C_H V_a[q_{sat}(T_s) - q_a] \quad (11)$$

Where L_v (J.kg^{-1}) is the latent heat of vaporization, , $q_{sat}(T_s)$ (kg.kg^{-1}) is the saturated specific humidity at the surface temperature T_s and q_a (kg.kg^{-1}) is the atmospheric specific humidity at the lowest atmospheric level. h_u is the relative humidity at the ground surface. δ is the vegetation fraction that covered by intercepted water. R_a and R_s (s.m^{-1}) are the aerodynamic and canopy surface resistances, respectively.

Additionally, in this study, ISBA uses the A-g_s parameterization to estimate the stomatal conductance g_s, by considering the impact of the atmospheric carbon dioxide concentration and the interactions between all environmental factors on the stomatal aperture. Therefore, the leaf stomatal conductance is expressed as follow (Calvet et al., 1998):

$$g_s = g_c + 1.6\left(A_n - A_{min}\left(\frac{D_s}{D^*_{max}}\frac{A_n+R_d}{A_m+R_d}\right) + R_d\left(1 - \frac{A_n+R_d}{A_m+R_d}\right)\right)/(C_s - C_i) \quad (12)$$

Where g_c (mm.s^{-1}) is the cuticular conductance, A_n (mg.m^{-2}.s^{-1}) is the net assimilation, $A_{\min}$ is the rate of the residual photosynthesis rate (at full light intensity). C_s and C_i are the internal and air CO_2 concentrations, respectively. D_s and D^*_{max} are the leaf-to-air saturation deficit and D^*_{max} the maximum leaf-to-air saturation deficit, respectively. A_m is the photosynthesis rate in light-saturating conditions.

The g_s is multiplied by the Leaf Area Index (LAI) value in order to scale up g_s from the leaf to the canopy. Finally, the integrated canopy net assimilation A_{nI} and conductance g_{sI} which were used to compute the heat and water vapor surface fluxes and the canopy resistance, respectively, are then written by assuming an homogeneous leaf vertical distribution as follows:

$$A_{nI} = LAI \int_0^1 A_n d(z/h) \quad (13)$$

$$g_{sI} = LAI \int_0^1 g_s d(z/h) \quad (14)$$

With h is the height of the canopy and z is the distance to the soil.

ISBA Multi-Energy Balance (MEB)

Compared to ISBA standard, MEB distinguishes the soil and the vegetation surface temperatures. Fluxes from the ground or vegetation first transit to the so called "canopy air space" or "canopy" before being in contact with the atmosphere. For an extended details about the prognostic equations and its numerical resolution aspects as well as the various assumptions of the MEB version, the reader can refer to Boone et al. (2017). We develop in the following paragraphs the main equations and parameterizations that will be used for this study. As soil freeze thaw is negligible for this study (no snow process involved), the related terms will be not presented.

The prognostic equations for the energy budget are:

$$C_v \frac{\partial T_v}{\partial t} = R_{nv} - H_v - LE_v \quad (15)$$

$$C_{g,1} \frac{\partial T_{g,1}}{\partial t} = R_{ng} - H_g - LE_g - G_{g,1} \quad (16)$$

Where $T_{g,1}$ is the uppermost ground temperature, and T_v is the bulk canopy temperature (K). The subscripts 1, v and g indicate the uppermost layer, vegetation canopy and ground. The ISBA-MEB sensible heat fluxes, H_v (between the vegetation and canopy air space), H_g (between the ground and canopy) and H_c (between the canopy and the overlaying atmosphere) are defined as:

$$H_v=\rho_a\frac{(\Gamma_v-\Gamma_c)}{R_{av-c}} \quad (17)$$

$$H_g=\rho_a\frac{(\Gamma_g-\Gamma_c)}{R_{ag-c}} \quad (18)$$

$$H_c=\rho_a\frac{(\Gamma_c-\Gamma_a)}{R_{ac-c}} \quad (19)$$

R_{ag-c}, R_{av-c} and R_{ac-a} are s the aerodynamic resistances to heat transfer between: the canopy and the ground (Choudhury and Monteith, 1988), the canopy and the vegetation and the atmosphere and the canopy, respectively. Γ (J.kg^{-1}) is a thermodynamic variable which is expressed as a linear relationship with the temperature (Boone et al., 2017). Note that in the model code, potential temperature or dry static energy are used as thermodynamic variables, but for simplicity, these quantities have been approximated using temperature (since the impact of this approximation is quite small in the current study).

The ISBA-MEB latent heat fluxes, E_v (between the vegetation and canopy), E_g (between the ground and canopy) and E_c (between the canopy and the overlaying atmosphere) are defined as:

$$E_v=\rho_a h_{sv}\frac{(q_{satv}-q_c)}{R_{av-c}} \quad (20)$$

$$E_g=\rho_a\frac{(q_g-q_c)}{R_{ag-c}} \quad (21)$$

$$E_c=\rho_a\frac{(q_c-q_a)}{R_{ac-a}} \quad (22)$$

Where h_{sv} is the Halstead coefficient.

In what follows, we present the main parameterizations introduced to calculate the new parameters needed by the model, as the fraction of the vegetation covered with intercepted water:

$$\delta_v=(1-\omega_{rv})\left(\frac{W_r}{W_{r\max}}\right)^{2/3}+\frac{\omega_{rv}W_r}{(1+\alpha_{rv}LAI)W_{r\max-\alpha_{rv}}W_r} \quad (23)$$

The maximum water interception storage on capacity on the vegetation is defined simply as:

$$W_{r\max}=c_{wrv}LAI \quad (24)$$

With C_{wrv} = 0.2

The canopy absorption is defined as:

$$\sigma_{LW} = 1 - \exp\left(-\tau_{LW} LAI\right) \quad (27)$$

Where τ_{LW} represents a longwave radiation transmission factor that can be species (or land classification) dependent.

The aerodynamic resistance between the vegetation canopy and the surrounding air space is defined as:

$$R_{avg-c} = \left(g_{av} + g_{av}^{*}\right)^{-1} \quad (28)$$

The bulk canopy aerodynamic conductance g_{av} between the canopy and the canopy air is parameterized as follows (Choudhury and Monteith, 1988):

$$g_{av} = \frac{2LAI\,\alpha_{av}}{\phi_v^{'}} \left(\frac{u_{hv}}{l_w}\right)^{1/2} \left[1 - \exp\left(-\phi_v^{'} / 2\right)\right] \quad (29)$$

Where u_{hv} is the wind speed at the top of the canopy (m.s^{-1}), l_w is the leaf width, α_{av} is the canopy conductance scale factor, ϕ'_v is the attenuation coefficient for wind.